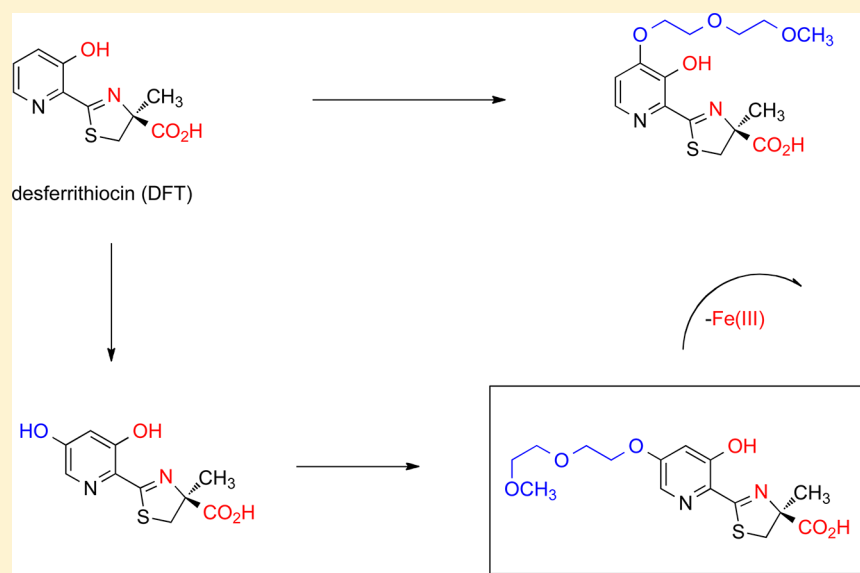


Substituent Effects on Desferrithiocin and Desferrithiocin Analogue Iron-Clearing and Toxicity Profiles

Raymond J. Bergeron,* Jan Wiegand, Neelam Bharti, and James S. McManis

Department of Medicinal Chemistry, University of Florida, Box 100485 JHMHC, Gainesville, Florida, 32610-0485

S Supporting Information



ABSTRACT: Desferrithiocin (DFT, **1**) is a very efficient iron chelator when given orally. However, it is severely nephrotoxic. Structure–activity studies with **1** demonstrated that removal of the aromatic nitrogen to provide desazadesferrithiocin (DADFT, **2**) and introduction of either a hydroxyl group or a polyether fragment onto the aromatic ring resulted in orally active iron chelators that were much less toxic than **1**. The purpose of the current study was to determine if a comparable reduction in renal toxicity could be achieved by performing the same structural manipulations on **1** itself. Accordingly, three DFT analogues were synthesized. The iron-clearing efficiency and ferrokinetics were evaluated in rats and primates; toxicity assessments were carried out in rodents. The resulting DFT ligands demonstrated a reduction in toxicity that was equivalent to that of the DADFT analogues and presented with excellent iron-clearing properties.

■ INTRODUCTION

Nearly all life forms require iron as a micronutrient. However, the low solubility of Fe(III) hydroxide ($K_{sp} = 1 \times 10^{-39}$),¹ the predominant form of the metal in the biosphere, required the development of sophisticated iron storage and transport systems in nature. Microorganisms utilize low molecular weight, ferric iron-specific ligands, siderophores;² eukaryotes tend to employ proteins to transport and store iron.^{3–5} Humans have evolved a highly efficient iron management system in which we absorb and excrete only about 1 mg of the metal daily; there is no mechanism for the excretion of excess metal.⁶ Whether derived from transfused red blood cells^{7–9} or from increased absorption of dietary iron,^{10,11} without effective treatment, body iron progressively increases with deposition in the liver, heart, pancreas, and elsewhere (iron overload disease).

In patients with iron overload disease, the toxicity derives from iron's interaction with reactive oxygen species.^{12–14} For

example, in the presence of Fe(II), endogenous H₂O₂ is reduced to the hydroxyl radical (HO•), a very reactive species, and HO[−], the Fenton reaction. The hydroxyl radical reacts very quickly with a variety of cellular constituents and can initiate free radicals and radical-mediated chain processes that damage DNA and membranes and produce carcinogens.^{13,15} The liberated Fe(III) is reduced back to Fe(II) via a variety of biological reductants (e.g., ascorbate, glutathione), a problematic cycle.

Iron-mediated damage can be focal, as in reperfusion damage,¹⁶ Parkinson's,¹⁷ Friedreich's ataxia,¹⁸ macular degeneration,¹⁹ and hemorrhagic stroke,²⁰ or global, as in transfusional iron overload, for example, thalassemia,²¹ sickle cell disease,^{21,22} and myelodysplasia,²³ with multiple organ involvement. The

Received: April 10, 2012

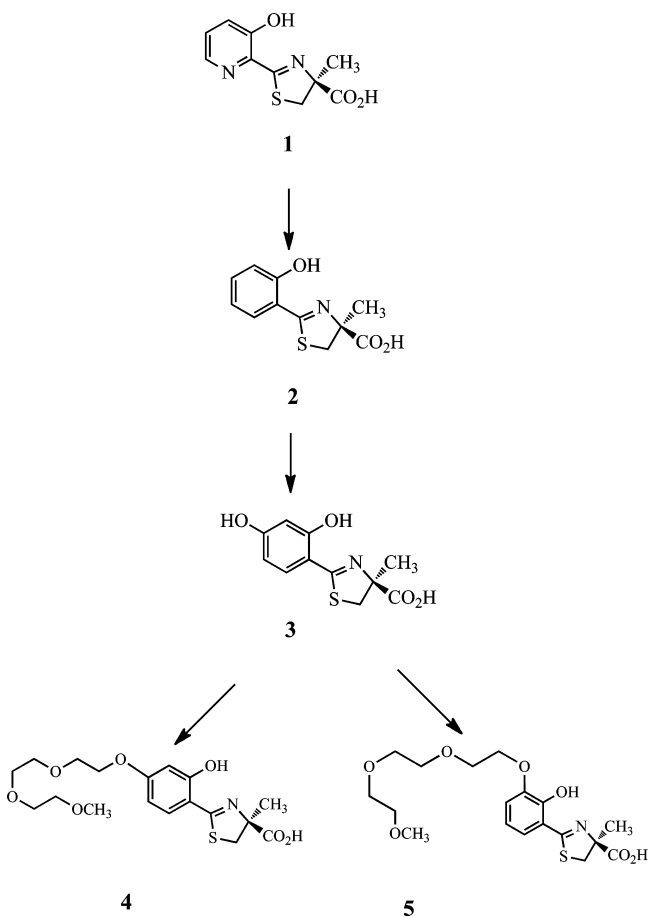
Published: August 13, 2012

solution in both scenarios is the same: chelate and promote the excretion of excess unmanaged iron.

Treatment with a chelating agent capable of sequestering iron and permitting its excretion from the body is the only therapeutic approach available.^{24,25} Some of the iron-chelating agents that are now in use or that have been clinically evaluated include desferrioxamine B mesylate (DFO),²⁶ 1,2-dimethyl-3-hydroxy-4-pyridinone (deferiprone, L1),^{27–30} and 4-[3,5-bis(2-hydroxyphenyl)-1,2,4-triazol-1-yl]benzoic acid (desferasirox, ICL670A).^{31–34} Each of these ligands presents with shortcomings. DFO must be given subcutaneously (sc) for protracted periods of time, for example, 12 h a day, 5 days a week, a serious patient compliance issue.^{7,35,36} Deferiprone, while orally active, simply does not remove enough iron to maintain patients in a negative iron balance.^{27–30} Desferasirox did not show non-inferiority to DFO and is associated with numerous side effects, including some serious renal toxicity issues.^{31–34}

In addition to the above chelators, two desferrithiocin [(S)-4,5-dihydro-2-(3-hydroxy-2-pyridinyl)-4-methyl-4-thiazolecarboxylic acid (DFT, **1**, Chart 1) analogues have made it to clinical

Chart 1. Extensive Structural Alterations of the Tridentate Chelator **1 Were Carried Out, Including Simple Hydroxylation of the Aromatic Ring of **2** To Yield **3**, or the Introduction of Polyether Fragments to **2**, For Example, **4** and (S)-4,5-Dihydro-2-[2-hydroxy-3-(3,6,9-trioxadecyloxy)]-4-methyl-4-thiazolecarboxylic Acid (**5**)**



trials. As will be described below, although **1** itself is severely nephrotoxic,³⁷ extensive structure–activity relationship (SAR) studies,^{38–40} including simple hydroxylation of the aromatic ring

of (S)-4,5-dihydro-2-(2-hydroxyphenyl)-4-methyl-4-thiazolecarboxylic acid (**2**, Chart 1) to yield (S)-2-(2,4-dihydroxyphenyl)-4,5-dihydro-4-methyl-4-thiazolecarboxylic acid (deferitricin, **3**,⁴¹ Chart 1), or the introduction of polyether fragments^{42,43} to **2**, for example, (S)-4,5-dihydro-2-[2-hydroxy-4-(3,6,9-trioxadecyloxy)]-4-methyl-4-thiazolecarboxylic acid (**4**, Chart 1), led to the discovery of orally active iron chelators that were much less toxic than **1**. This begs the question of what the impact of the hydroxylation of DFT itself, or fixing a polyether fragment to DFT, would have on the nephrotoxicity and iron clearance properties of the new analogues.

RESULTS AND DISCUSSION

Design Concept. DFT (**1**, Table 1) is a natural product iron chelator isolated from *Streptomyces antibioticus*.⁴⁴ It forms a 2:1 complex with Fe(III) with a cumulative formation constant of $4 \times 10^{29} \text{ M}^{-1}$.^{45,46} Although the compound was shown to be an excellent deferration agent when administered orally (po) to rats⁴⁷ and primates,^{48,49} it caused severe nephrotoxicity in rats.³⁷ However, the compound's oral activity spurred SAR studies focused on the DFT platform aimed at identifying an orally active and safe DFT analogue.^{38–40}

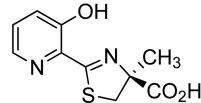
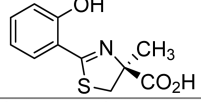
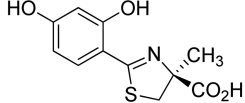
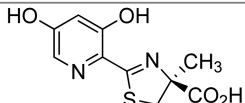
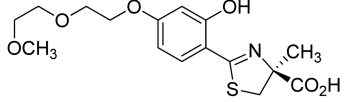
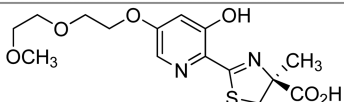
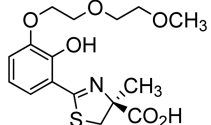
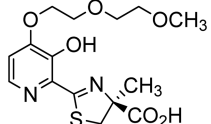
Our approach first entailed simplifying the platform. Removal of the pyridine nitrogen of **1** provided **2** (Chart 1 and Table 1), the parent ligand of the desazadesferrithiocin (DADFT) series.⁴⁰ Interestingly, although **2** was not overtly nephrotoxic, it elicited serious gastrointestinal (GI) problems.^{37,38,40} In spite of its GI toxicity, the ligand's excellent iron-clearing efficiency (ICE) and the absence of nephrotoxicity prompted further SAR studies predicated on this pharmacophore. This led to the discovery that the lipophilicity (partition between octanol and water, expressed as the log of the fraction in the octanol layer, $\log P_{\text{app}}$)⁵⁰ of the DADFT analogues could have a profound effect on the ligand's ICE, organ distribution, and toxicity profile.^{38,51,52}

Ultimately, it was determined that hydroxylation of DADFT and a number of different analogues in the 3'-, 4'-, or 5'-position allowed for ligands that were very efficient, orally active iron chelators with profoundly less toxicity than **1** or **2**.^{38,51} Clearly, hydroxylation had a significant effect on toxicity reduction. One of these ligands, **3**, was taken into human clinical trials by Genzyme and was moving forward until the once daily dosing was changed to twice daily.⁴¹ Patients presented with increases in blood urea nitrogen (BUN) and serum creatinine (SCr) levels, and the trial was terminated.⁴¹

The molecule (**3**) was reengineered, introducing a 3,6,9-trioxadecyloxy group in the 4'-position of **2** (**4**, Chart 1).⁴² This provided a remarkably efficient orally active iron chelator, which, given to rats po once or twice daily, was virtually nephrotoxicity-free.⁴² This turned out also to be true when a variety of polyether backbones were fixed at the 3'-, 4'-, or 5'-position of the DADFT pharmacophore.^{43,53–55} In fact, (S)-4,5-dihydro-2-[2-hydroxy-3-(3,6,9-trioxadecyloxy)]-4-methyl-4-thiazolecarboxylic acid (**5**, Chart 1) has now been moved forward to clinical trials. Thus, it appeared as though fixing a polyether fragment to the DADFT framework was also a uniformly effective tool in further reducing **3**-induced nephrotoxicity. These observations drive the current study.

A series of questions based on the results of the SAR studies of DADFT analogues are addressed as follows: (1) How does hydroxylation of **1** itself affect its iron-clearing properties? (2) How does hydroxylation of **1** affect its renal toxicity? (3) What is the effect of fixing polyether fragments to **1** on its iron clearance? (4) What is the effect of fixing polyether fragments to **1** on its

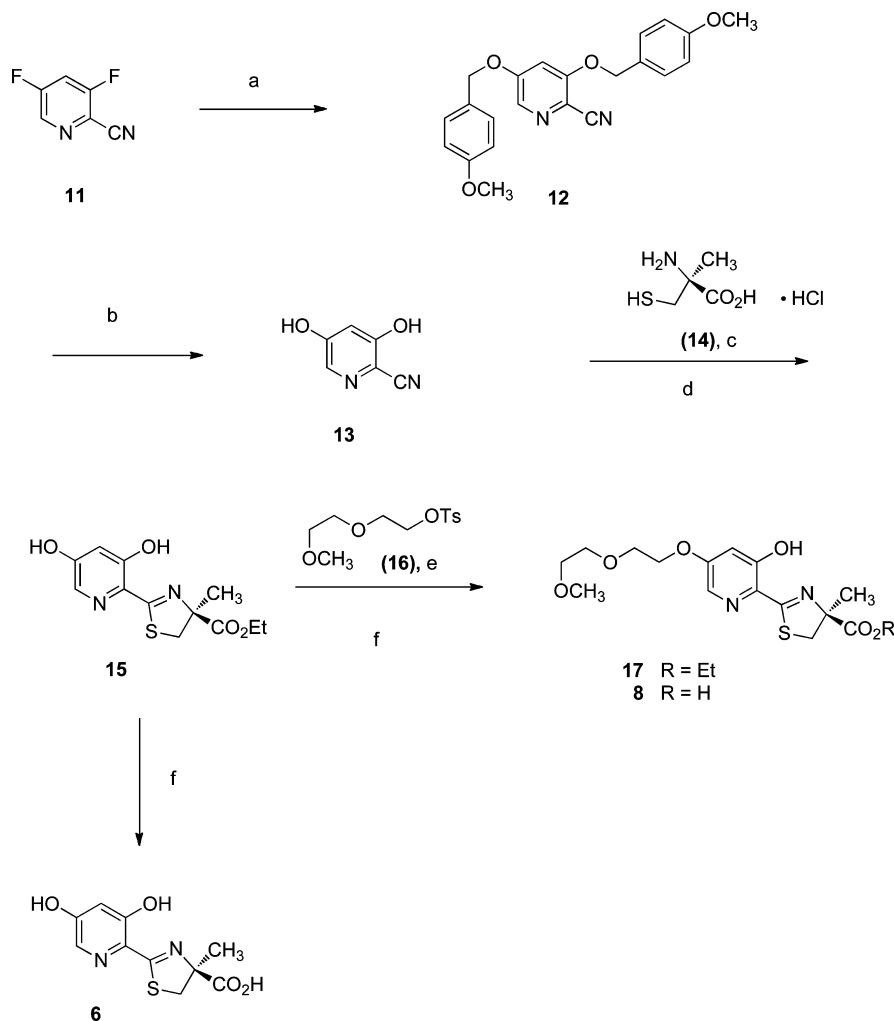
Table 1. Iron-Clearing Efficiency of DFT Analogues Administered to Rodents and Primates with the Respective Log P_{app} Values

Chelator	Comp. No.	Rodent Iron-Clearing Efficiency ^a (%)	Primate Iron-Clearing Efficiency ^c (%)	Log P_{app}	PR ^d
	1	5.5 ± 3.2 [93/7]	16.1 ± 8.5 [78/22]	-1.77	2.9
	2	2.7 ± 0.5 [100/0]	21.5 ± 12.0 [76/24]	-0.34	8.0
	3	1.1 ± 0.8 [100/0]	16.8 ± 7.2 [88/12]	-1.05	15.3
	6	9.0 ± 3.8 [97/3]	10.0 ± 2.9 [58/42]	-1.68	1.1
	7	26.7 ± 4.7 ^b [97/3]	26.3 ± 9.9 [93/7] (capsule) 28.7 ± 12.4 [83/17] (sodium salt)	-0.89	1.0 1.1
	8	11.7 ± 1.2 [97/3]	18.0 ± 5.2 [63/37]	-1.59	1.5
	9	15.1 ± 2.0 ^b [99/1]	22.5 ± 6.4 [86/14]	-0.96	1.5
	10	14.2 ± 2.4 [98/2]	6.1 ± 1.8 (po) [40/60] 16.9 ± 7.3 (sc) [64/36]	-1.38	0.4 1.2

^aIn the rodents [$n = 3$ (7), 4 (2 and 10), 5 (1, 6, 8, and 9), or 8 (3)], the drugs were given po at a dose of 150 (1 and 2) or 300 $\mu\text{mol/kg}$ (3 and 6–10). The drugs were administered in capsules (7), solubilized in 40% Cremophor RH-40/water (1 and 2), or given as their monosodium salts, prepared by the addition of 1 equiv of NaOH to a suspension of the free acid in distilled water (3, 6, and 8–10). The efficiency of each compound was calculated by subtracting the 24 or 48 h iron excretion of control animals from the iron excretion of the treated animals. The number was then divided by the theoretical output; the result is expressed as a percent. The relative percentages of the iron excreted in the bile and urine are in brackets. The ICE data for 1 is from ref 47, 2 is from ref 38, 3 is from ref 51, 7 is from ref 54, and 9 is from ref 55. ^bICE is based on a 48 h sample collection period. ^cIn the primates [$n = 4$ (1, 2, 6, and 7 in capsules and 8–10), or 6 (3), or 7 (7 as the monosodium salt)], the chelators were given po at a dose of 75 (2 and 6–10) or 150 $\mu\text{mol/kg}$ (1 and 3). Ligand 10 was also given to the primates sc at a dose of 75 $\mu\text{mol/kg}$. The drugs were administered in capsules (7), solubilized in 40% Cremophor RH-40/water (1 and 2), or given as their monosodium salts, prepared by the addition of 1 equiv of NaOH to a suspension of the free acid in distilled water (1–3 and 6–10). The efficiency was calculated by averaging the iron output for 4 days before the drug, subtracting these numbers from the 2 day iron clearance after the administration of the drug, and then dividing by the theoretical output; the result is expressed as a percent. The ICE data for 1–3 are from ref 38, 7 is from ref 54, and 9 is from ref 55. The relative percentages of the iron excreted in the feces and urine are in brackets. ^dThe performance ratio (PR) is defined as the mean $\text{ICE}_{\text{primates}}/\text{ICE}_{\text{rodents}}$.

renal toxicity? To answer these questions, three ligands were assembled (Table 1), (S)-4,5-dihydro-2-(3,5-dihydroxy-2-pyridinyl)-4-methyl-4-thiazolecarboxylic acid (6), (S)-4,5-dihydro-2-[3-hydroxy-5-(3,6-dioxahexyloxy)-2-pyridinyl]-4-methyl-4-thiazolecarboxylic acid (8), and (S)-4,5-dihydro-2-[3-hydroxy-4-(3,6-dioxahexyloxy)-2-pyridinyl]-4-methyl-4-thiazolecarboxylic acid (10).

Synthesis. The preparation of 5'-hydroxydesferrithiocin (6) and its 5'-nor polyether (8) (Table 1) began with 2-cyano-3,5-difluoropyridine (11), which was converted to 2-cyano-3,5-dihydroxypyridine (13) in two steps (Scheme 1). Heating 11 with 4-methoxybenzyl alcohol in the presence of NaH (2.5 equiv each) in DMF^{56,57} at 95 °C for 18 h gave protected diol 12 in 73% yield. Removal of the 4-methoxybenzyl groups of 12 using

Scheme 1. Synthesis of 6 and 8^a

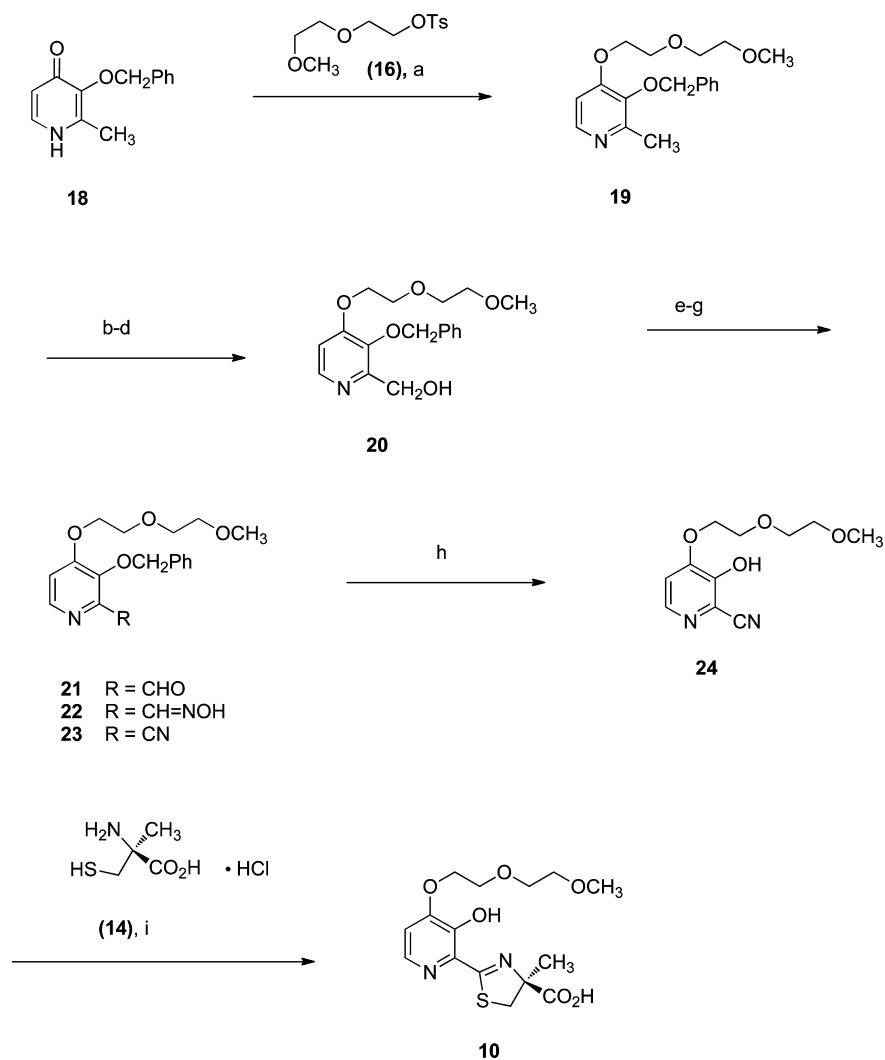
^aReagents and conditions: (a) 4-Methoxybenzyl alcohol, 60% NaH (2.5 equiv each), DMF, 95–100 °C, 18 h, 73%. (b) TFA, pentamethylbenzene, 22 h, quantitative. (c) CH₃OH, 0.1 M pH 6 buffer, NaHCO₃, 73–76 °C, 45 h. (d) EtI, DIEA (1.5 equiv each), DMF, 47 h, 70%. (e) K₂CO₃ (1.6 equiv), acetone, reflux, 1 d, 65%. (f) 50% NaOH(aq), CH₃OH, then HCl, 96% (6), 97% (8).

excess trifluoroacetic acid (TFA)⁵⁸ and pentamethylbenzene⁵⁹ at room temperature for 22 h provided nitrile 13 in quantitative yield. Cyclocondensation of 13 with (*S*)-2-methyl cysteine (14) in aqueous CH₃OH buffered at pH 6 at 75 °C for 45 h followed by esterification of crude acid 6 with iodoethane and *N,N*-diisopropylethylamine (DIEA) (1.5 equiv each) in DMF produced ethyl (*S*)-4,5-dihydro-2-(3,5-dihydroxy-2-pyridinyl)-4-methyl-4-thiazolecarboxylate (15) in 70% yield. Hydrolysis of 15 with aqueous NaOH in CH₃OH at room temperature generated 6 as a solid in 96% yield. Also, ester 15 was alkylated at the less hindered phenol⁵⁴ in the presence of the pyridine nitrogen with tosylate 16 and K₂CO₃ in refluxing acetone, affording ligand precursor 17 in 65% yield. The carboxylate was unmasked under alkaline conditions to give 8 in 97% yield as an oil.

Synthesis of the 4'-nor polyether DFT analogue 10, an isomer of iron chelator 8 (Table 1), started with 2-methyl-3-(benzyloxy)-4-pyridone (18), available in two steps from maltol⁶⁰ (Scheme 2). O-Alkylation of 18 with tosylate 16 and K₂CO₃ in refluxing acetonitrile⁶¹ afforded 2-methyl-3-(benzyloxy)-4-(3,6-dioxaheptyloxy)pyridine (19) in 68% yield. The methyl group of 19 was oxidized by known methodology,⁶⁰

providing aldehyde 21. Specifically, 19 was treated with 3-chloroperbenzoic acid (*m*-CPBA) in CH₂Cl₂, and the resulting *N*-oxide was heated at reflux in acetic anhydride. Cleavage of the acetate ester with base gave the 2-pyridinemethanol 20 in 87% overall yield. Primary alcohol 20 was further oxidized to aldehyde 21 in 83% yield with sulfur trioxide–pyridine complex and NEt₃ in DMSO and CHCl₃. The oxime 22, generated in 90% yield under standard conditions,⁴² was heated at reflux with acetic anhydride, furnishing the corresponding nitrile 23 in 94% yield. Removal of the benzyl-protecting group from 23 by hydrogenolysis (1 atm, 10% Pd–C, CH₃OH) in the presence of the cyano group and pyridine ring produced 4-(3,6-dioxaheptyloxy)-3-hydroxy-2-pyridinecarbonitrile (24) in 85% yield. Heating 24 with amino acid 14 in aqueous CH₃OH buffered at pH 6 generated 10 in 95% yield.

Stoichiometry of the Ligand–Fe(III) Complexes. Earlier studies with 1 by Andregg and Råber showed the chelator to form a 2:1 complex with Fe(III).⁴⁶ The cumulative formation constant for this complex was determined to be $4 \times 10^{29} \text{ M}^{-1}$. Hahn et al. were ultimately able to isolate both the Δ and λ 1–Cr(III) complexes, with chromium serving as a surrogate for Fe(III).⁴⁵ As expected, the crystal structures of the complexes

Scheme 2. Synthesis of 10^a

^aReagents and conditions: (a) K_2CO_3 (2 equiv), CH_3CN , 68%. (b) *m*-CPBA, CH_2Cl_2 . (c) Ac_2O , reflux. (d) $NaOH(aq)$, $EtOH$, reflux, 4 h, 87%. (e) SO_3 , pyridine, NEt_3 , $DMSO$, $CHCl_3$, 16 h, 83%. (f) $H_2NOH \cdot HCl$, $NaOAc$, CH_3OH , reflux, 2 h, 90%. (g) Ac_2O , reflux, 94%. (h) H_2 , 10% $Pd-C$, CH_3OH , 85%. (i) CH_3OH , 0.1 M pH 6 buffer, $NaHCO_3$, 75 °C, 48 h, 95%.

unequivocally demonstrated a 2:1 ligand to metal ratio. In later studies in our laboratories, Job's plots with **3**³⁸ (Table 1) and the corresponding desmethyl analogue⁴⁰ also showed that these ligands formed 2:1 complexes with Fe(III). This is of course in keeping with the fact that the donor groups of the chelators, the aromatic hydroxyl, the thiazoline nitrogen, and the carboxylate are the same as in **1** itself. Furthermore, the cumulative distance (9.77 Å) between the donor groups in our x-ray crystal structure of free ligand **3**⁶² is identical to the corresponding value in the Cr(III) complex of **1**.⁴⁵ In the current study, Job's plots were run on **6**, **8**, and **10** (Figure 1). In each instance, the ligands formed 2:1 complexes with Fe(III).

Partition Properties. The partition values between octanol and water (at pH 7.4, Tris buffer) were determined using a "shake flask" direct method of measuring $\log P_{app}$ values.⁵⁰ The fraction of drug in the octanol is then expressed as $\log P_{app}$. While the values vary widely (Table 1), one observation stands out: DFT and its analogues are always more hydrophilic than their DADFT counterparts, that is, **1** vs **2**, **6** vs **3**, **8** vs **7**, and **10** vs **9**. This, of course, is likely due to the presence of the aromatic nitrogen, a moderately good hydrogen bond acceptor, on the DFT

analogues. Relative to the differences in lipophilicity between DFT and DADFT, fixing a polyether backbone to either the DFT or the DADFT pharmacophore had a much more moderate effect (Table 1).

Chelator-Induced Iron Clearance in Noniron-Overloaded Bile Duct-Cannulated Rodents. A measure of the amount of iron excretion induced by a chelator is best described by its ICE. The ICE, expressed as a percent, is calculated as (ligand-induced iron excretion/theoretical iron excretion) \times 100. To illustrate, the theoretical iron excretion after administration of 1 mmol of DFO, a hexadentate chelator that forms a 1:1 complex with Fe(III), is 1 milli-g-atom of iron. Two millimoles of DFT (**1**, Table 1), a tridentate chelator that forms a 2:1 complex with Fe(III), is required for the theoretical expression of 1 milli-g-atom of iron.

The ICE values for compounds **1–3**, **7**, and **9** (Table 1) are historical and included for comparative purposes.^{38,42,47,54,55} The biliary ferrokinetics profiles of ligands **3** and **6–10** are presented in Figure 2. Each of the rats in these studies was given a single po dose of the chelator at 300 μ mol/kg. Note that the biliary ferrokinetics data for compounds **1** and **2** are not

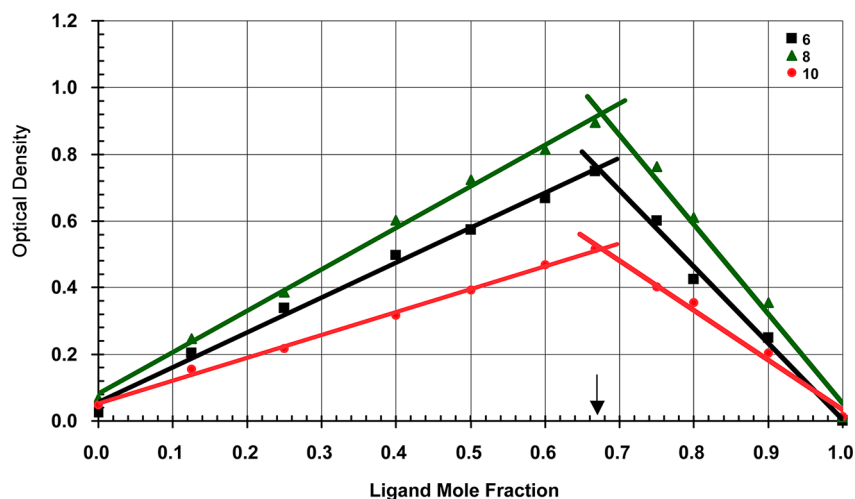


Figure 1. Job's plots of the Fe(III) complexes of ligands 6, 8, and 10. Solutions containing different ligand/Fe(III) ratios were prepared such that $[\text{ligand}] + [\text{Fe(III)}] = 1.0 \text{ mM}$ in Tris-HCl buffer at pH 7.4. The theoretical mole fraction maximum for a 2:1 ligand:Fe complex is 0.667 (arrow). The observed maxima for 6, 8, and 10 are 0.669, 0.676, and 0.677, respectively. The optical density (y -axis) was determined at 498, 484, and 485 nm for 6, 8, and 10, respectively.

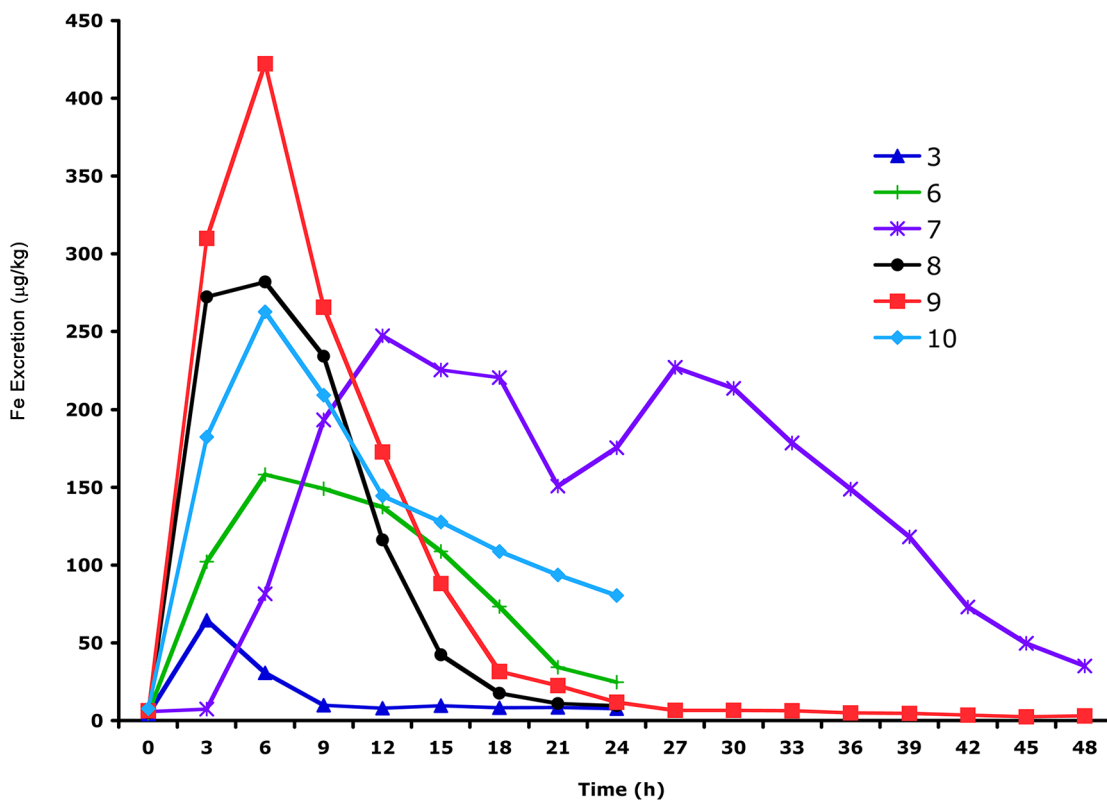


Figure 2. Biliary ferrokinetics of DFT analogues (6, 8, and 10) and DADFT analogues (3, 7, and 9) in bile duct-cannulated rats. The compounds were given po at $300 \mu\text{mol/kg}$. The iron excretion (y -axis) is reported as μg of iron per kg body weight.

included, simply because these animals were dosed at $150 \mu\text{mol/kg}$ and the curves are not strictly comparable with the $300 \mu\text{mol/kg}$ data. Although these results are published elsewhere,^{38,47} we will comment on this briefly.

DFT (**1**) given to the rats po at a dose of $150 \mu\text{mol/kg}$ had an ICE of $5.5 \pm 3.2\%$.⁴⁷ Maximum iron clearance (MIC) occurred at 3 h, but deferration had returned to baseline levels by 12 h. The desaza analogue of DFT, **2**, at $150 \mu\text{mol/kg}$ had an ICE of $2.7 \pm 0.5\%$.³⁸ The ligand reached MIC at 6 h and had returned to baseline iron excretion by 12 h postdrug.

Compound **3** was the least effective ligand, with an ICE of $1.1 \pm 0.8\%$.⁴² It presented with an MIC at 3 h; deferration was virtually over at 9 h (Figure 2). The DFT analogue of **3**, ligand **6**, had an ICE that was significantly better than **3**, $9.0 \pm 3.8\%$ ($p < 0.005$). MIC occurred at 6 h, and its iron decorporation slowly dropped to near baseline levels by 24 h. The most efficient chelator, **7**, had an ICE of $26.7 \pm 4.7\%$.⁵⁴ The ligand also had a very protracted iron clearance; even though its MIC occurred at around 12 h, it was still active at 48 h. Note that although the biliary ferrokinetics curve of **7** may appear to be biphasic

(Figure 2), the reason for this unusual line shape is that several animals had temporarily obstructed bile flow. While the concentration of iron in the bile remained the same, the bile volume, and thus overall iron excretion, decreased. Once the obstruction was resolved, bile volume and overall iron excretion normalized.

The DFT analogue **8** had an ICE that was significantly less than that of **7** (11.7 ± 1.2 vs $26.7 \pm 4.7\%$ for **8** and **7**, respectively, $p < 0.02$). Ligand **8** also achieved MIC earlier than **7**, 6 vs 12 h (Figure 2), and the iron clearance induced by **8** was basically over by 21 h. In addition, DADFT analogue **9**⁵⁵ and its corresponding DFT analogue **10** presented with similar ICEs ($\sim 15\%$) but with very different biliary ferrokinetics (Figure 2). Both ligands achieved MIC at 6 h. However, while ligand **9**-induced iron clearance had returned to baseline by 24 h, **10** was still quite active.

Finally, there is an excellent correlation between ICE and $\log P_{app}$ in rodents among the DFT analogues **6**, **8**, and **10** (Figure 3). The most lipophilic ligands are also the most

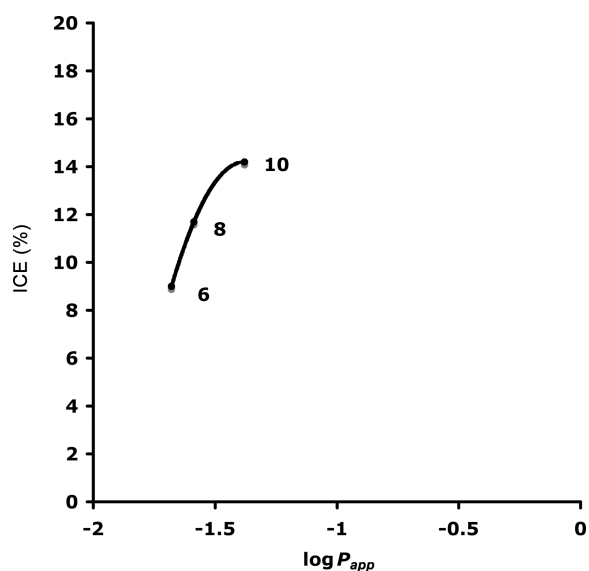


Figure 3. ICE, expressed as a percentage (y-axis), vs $\log P_{app}$ for DFT analogues **6**, **8**, and **10** in bile duct-cannulated rats given po at a dose of 300 $\mu\text{mol/kg}$.

active. We have observed this ICE vs $\log P_{app}$ pattern time and again.^{38,51,52}

Chelator-Induced Iron Clearance in Iron-Overloaded Primates. The primate iron clearance data are provided in Table 1. The ICE values for compounds **1**, **2**, **3**, **7**, and **9** are again historical and included for comparative purposes.^{38,54,55} The chelators were given to the primates po at a dose of 75 (**2** and **6–10**) or 150 $\mu\text{mol/kg}$ (**1** and **3**); **10** was also given to the primates sc at a dose of 75 $\mu\text{mol/kg}$. Ligand **1** was found to have an ICE of $6.1 \pm 8.5\%$.³⁸ Removal of the pyridine nitrogen to yield **2** increased the ICE to $21.5 \pm 12\%$.³⁸ However, the increase in ICE was not significant ($p > 0.05$). The introduction of a hydroxyl group at the 4'-position of **2** to provide analogue **3** resulted in a chelator with an ICE of $16.8 \pm 7.2\%$,³⁸ which is within error of the ICE found for **1** and **2** ($p > 0.05$). The reintroduction of the pyridine nitrogen into DADFT ligand **3** to provide DFT analogue **6** (Table 1) decreased the ICE to $10.0 \pm 2.9\%$, significantly less than its DADFT counterpart, **3** ($p < 0.05$). When a polyether fragment was attached to the 5'-position of **6** to yield **8**, the ICE increased to $18.0 \pm 5.2\%$, again less than that

achieved by the corresponding DADFT ligand **7**. Likewise, the ICE of **10** given po was also less than that of DADFT analogue **9** (Table 1). In fact, the DADFT analogues were consistently better deferrating agents in the primates than the corresponding DFT ligands (Table 1).

Several generalizations can be derived from Table 1. The performance ratios, PR values, $\text{ICE}_{\text{primate}}/\text{ICE}_{\text{rodent}}$ (Table 1), show that the ligands are either as effective or better at iron clearance in primates than in rodents. The exception to this is ligand **10**. The ICE of this drug given po to the primates is $6.1 \pm 1.8\%$, while in the rats, it is $14.2 \pm 2.4\%$. Its PR ratio was 0.4, showing it to be far less efficient in primates than rodents. The poor iron clearance in primates relative to rodents was surprising. Two scenarios were evaluated in search of an explanation: ligand–plasma binding and a potential GI absorption problem.

A ligand–plasma binding experiment was performed in which rodent and primate plasma were incubated separately with chelator **10** at 37 °C for 4 h. Each sample was then passed through a Millipore Amicon Ultra regenerated cellulose filter (3000 MWCO). The filtrate was assayed for **10**. The results indicated there was little, if any, binding of the ligand to either the rodent or the primate plasma. This suggests that ligand–plasma binding does not explain the difference in the rodent vs primate ICE values. However, when primates were given ligand **10** sc, the ICE rose to $16.9 \pm 7.3\%$, which is similar to what was seen in rodents given **10** orally (Table 1). This observation is consistent with the idea that the primates do not absorb **10** well when the drug is administered orally.

Effect of Hydroxylation or Introduction of a Polyether Fragment on DFT Toxicity. In a previous study, **1** was given to rats with normal iron stores po once daily at a dose of 384 $\mu\text{mol/kg/day}$ (100 mg/kg/day). All of the rats were dead by day 5 of a planned 10 day experiment. The chelator was found to be severely nephrotoxic.³⁷ The pathologist noted vacuolar changes of the proximal tubules that were diffuse and severe, with multifocal vacuolar degeneration and necrosis. Nevertheless, the drug's remarkable oral activity initiated a series of SAR studies aimed at the development of orally active, nontoxic DFT analogues. This led to the development of **3** (Table 1), which made it to clinical trials.⁴¹ This chelator, when given once daily, cleared iron from the patients and was proceeding forward. Unfortunately, it was discovered that the drug induced proximal tubule nephrotoxicity when it was administered twice daily, and the trial was halted.⁴¹ The chelator was reengineered, and it was determined that by fixing polyether fragments to the 3'- or 4'-position of **2**, for example, **5** and **4** (Chart 1), **7** (Table 1), the renal toxicity virtually disappeared.^{42,53–55} This outcome suggested that the introduction of either a hydroxyl group or a polyether fragment directly into DFT itself might reduce the drug's nephrotoxicity. Accordingly, ligands **6**, **8**, and **10** were synthesized and evaluated for their toxicity in rodents relative to **1**.

Assessment of chelator-induced impaired renal function has traditionally relied on the detection of a rise in BUN and/or SCr. However, because of the functional reserve of the kidney, these parameters are often unreliable indicators of acute kidney injury; the ultimate answer requires histopathology. The Critical Path Institute's Preventive Safety Testing Consortium (PSTC) has identified kidney injury molecule-1 (Kim-1, rat) or (KIM-1, human) as an early diagnostic biomarker for monitoring acute kidney tubular toxicity.⁶³ Kim-1 is a type 1 transmembrane protein located in the epithelial cells of proximal tubules.^{64,65} After injury, for

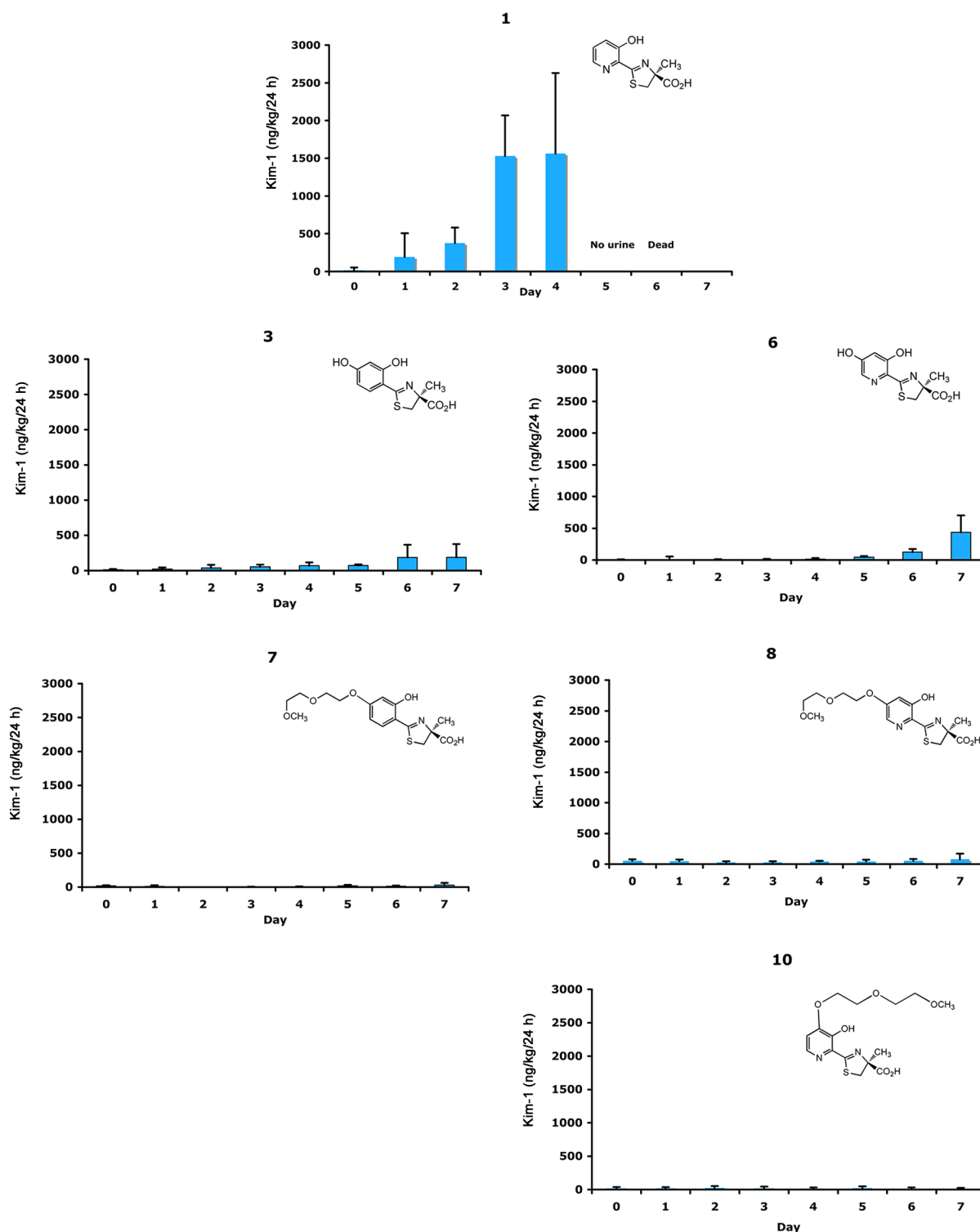


Figure 4. Urinary Kim-1 excretion (y-axis) is expressed as Kim-1 (ng/kg/24 h) of rats treated with DFT (**1**), DFT analogues **6**, **8**, and **10** or DADFT analogues **3** and **7**. The rodents were given the drugs po twice daily (b.i.d.) at a dose of 237 $\mu\text{mol/kg/dose}$ (474 $\mu\text{mol/kg/day}$) for up to 7 days. Note that none of the rats survived the planned 7 day exposure to **1**. $N = 5$ for **1**, **6–8**, and **10**; $N = 3$ for ligand **3**.

example, exposure to a nephrotoxic agent or ischemia, the ectodomain of Kim-1 is shed from the proximal tubular kidney epithelial cells into the urine.^{66–68} BioAssay Works has recently developed RenaStick, a direct lateral flow immunochromatographic assay, which allows for the rapid detection (less than 30 min) and quantitation of urinary Kim-1 (rat) or KIM-1 (human) excretion.⁶⁹ In the current

study, rats were treated with **1**, **6**, **8**, and **10** given po twice daily at a dose of 237 $\mu\text{mol/kg/dose}$ (474 $\mu\text{mol/kg/day}$) for up to 7 days. Urinary Kim-1 levels were assessed at 24 h intervals (Figure 4). The studies were performed on rats with normal iron stores; each animal served as its own control. The data for ligands **3** and **7** are historical and are included for comparative purposes.⁵⁵

None of the **1**-treated rats ($n = 5$) survived the planned 7 day exposure to the drug. Two rats became moribund and were sacrificed after being given the drug for 4 days. The three remaining animals were found dead the morning of day 6; they had received the chelator for 5 days. None of the rodents produced any urine on day 5. The **1**-treated rats' baseline (day 0) urinary Kim-1 value was <20 ng/kg/24 h (Figure 4). After 1 day of **1**, the Kim-1 had increased nearly 10-fold, to 192 ± 316 ng/kg/24 h. After 3 days of **1**, the Kim-1 had further increased to 1528 ± 539 ng/kg/24 h. Blood was taken from the two moribund animals immediately prior to sacrifice; the serum was assessed for its BUN and SCr content. The rats' BUN was 139 ± 8 mg/dL (normal 9–30 mg/dL),⁷⁰ while their SCr was 5.1 ± 0.3 mg/dL (normal 0.4–1 mg/dL).⁷⁰ In addition, as no blood was obtained from the three animals that were found dead, these values likely underestimate the actual impact of **1** on these parameters.

In contrast, in a previous study assessing the impact of **3** po on urinary Kim-1 excretion,⁵⁵ all of the treated rats ($n = 3$) survived the $237 \mu\text{mol/kg}$ twice daily ($474 \mu\text{mol/kg/day}$) \times 7 day dosing period. The rats' baseline (day 0) urinary Kim-1 content was <20 ng/kg/24 h (Figure 4). After 3 days of exposure to **3**, the urinary Kim-1 had increased to 69 ± 47 ng/kg/24 h. At the end of the 7 day dosing period, the urinary Kim-1 had further increased to 189 ± 187 ng/kg/24 h (Figure 4). The rats were euthanized on day 8; their BUN at that time was 32 ± 13 mg/dL, while their SCr was 1.3 ± 1.0 mg/dL.

In the current study, all of the animals treated po with the corresponding hydroxylated DFT analogue, **6**, at $237 \mu\text{mol/kg}$ twice daily ($474 \mu\text{mol/kg/day}$) also survived the full 7 days of treatment. The rats' baseline (day 0) urinary Kim-1 content was <20 ng/kg/24 h and remained <50 ng/kg/24 h until day 5 (Figure 4). On day 6, the Kim-1 increased to 125 ± 48 ng/kg/24 h and further increased to 435 ± 269 on day 7 (Figure 4). Although the increase in Kim-1 is greater with the **6**-treated rats than with the **3**-treated animals, the increase is not statistically significant ($p > 0.05$). The animals were euthanized on day 8; their BUN at that time was 13 ± 2 mg/dL, while their SCr was 0.5 ± 0.1 mg/dL. Thus, simple hydroxylation of the aromatic ring of both DADFT and DFT, for example, **3** and **6**, respectively, resulted in ligands that were much less toxic than DFT itself.

We previously demonstrated that introducing a polyether fragment in the 3'- or 4'-position of the DADFT pharmacophore provided remarkably efficient orally active iron chelators that were much less toxic than **3**.^{42,43,53–55} For example, the impact of ligand **7** on urinary Kim-1 excretion was determined when the drug was given po: (1) once daily during the course of 28 day toxicity trials, (2) once daily at a dose of $384 \mu\text{mol/kg/day}$ \times 10 days, and (3) twice daily at a dose of $237 \mu\text{mol/kg/dose}$ ($474 \mu\text{mol/kg/day}$) \times 7 days.⁵⁵ All of the rats survived the dosing period. The rats' baseline (day 0) urinary Kim-1 content was <20 ng/kg/24 h and stayed within error of this value for the duration of the drug exposure. The data from the $237 \mu\text{mol/kg}$ twice daily ($474 \mu\text{mol/kg/day}$) \times 7 days regimen⁵⁵ are depicted in Figure 4. In addition, the BUN and SCr of all of the 7-treated rats were well within the normal range.

In the current study, we evaluated the impact that affixing a polyether fragment to DFT itself would have on nephrotoxicity. Accordingly, groups of rats ($n = 5$) were given **8** or **10** po twice daily at $237 \mu\text{mol/kg/dose}$ ($474 \mu\text{mol/kg/day}$) \times 7 days. All of the animals survived the drug-dosing regimen. The animals' urinary Kim-1 excretion remained within error of that of the baseline (day 0) levels (Figure 4). In addition, the BUN and SCr

of all of the **8**- or **10**-treated rats were well within the normal range. Thus, as with the DADFT pharmacophore, fixing a polyether fragment to the DFT framework was an effective tool in further reducing nephrotoxicity.

CONCLUSION

We previously demonstrated that the severe nephrotoxicity associated with **1** could be ameliorated by the removal of the pyridine nitrogen of **1** to provide **2** and simple hydroxylation of the aromatic ring of **2** to yield **3** (Chart 1).^{38,51} Further reduction in **3**-induced nephrotoxicity, observed when the chelator was given po at $237 \mu\text{mol/kg}$ twice daily, was accomplished by the addition of polyether fragments, for example, **4**, **5**, and **7** (Chart 1 and Table 1).^{42,53–55} The purpose of the current study was to determine how these same structural modifications to DFT itself would impact the new ligands' ICE and nephrotoxicity. Accordingly, three DFT analogues, **6**, **8**, and **10**, were synthesized and assessed for their lipophilicity, ICE properties in rats and primates, and their toxicity in rats.

DFT (**1**, Table 1) and its analogues were all significantly more water-soluble (lower $\log P_{\text{app}}$) than the corresponding DADFT analogues, for example, **1** vs **2**, **6** vs **3**, **8** vs **7**, and **10** vs **9**. There was an excellent correlation between ICE and $\log P_{\text{app}}$ in rodents among the DFT analogues **6**, **8**, and **10** (Figure 3), with the more lipophilic ligands having a greater ICE. This trend is in keeping with previous observations that more lipophilic ligands have better ICE properties. The biliary ferrokinetics of the DFT and DADFT ligands in the bile duct-cannulated rats (Figure 2) have similar temporal properties, except for ligand **7**. This drug has the highest ICE and a very protracted iron clearance time.

In the primates, the DADFT analogues were consistently better deferration agents than the corresponding DFT ligands (Table 1). The most unusual finding was with ligand **10**, a DFT analogue with a 4'-(3,6-dioxaheptyloxy) ether functionality fixed to the 4'-position of **1**. When the drug was given po to the primates, its ICE was only 6.1 ± 1.8 vs $14.2 \pm 2.4\%$ in the rats and a PR value of 0.4 (Table 1). However, when the monkeys were given the chelator sc, its ICE increased to $16.9 \pm 7.3\%$, with a PR value now at 1.2. This is consistent with the idea that ligand **10** simply was not absorbed well orally in primates.

The effects of structural modification of DFT on its renal toxicity were assessed in rats using a urinary Kim-1 (kidney injury molecule) assay,⁶⁹ as well as monitoring BUN and SCr. The most notable finding was that fixing a hydroxyl group or a polyether fragment to the DFT aromatic ring resulted in a nearly identical reduction in renal toxicity as seen after the same modification to DADFT (Figure 4). Although some nephrotoxicity was noted with both hydroxylated DADFT and DFT analogues, **3** and **6**, respectively, the introduction of polyether groups into either pharmacophore resulted in ligands with little to no impact on renal function, for example, **7**, **8**, and **10** (Figure 4).

In summary, rather simple manipulation of the DFT aromatic ring, for example, hydroxylation, or the introduction of a polyether functionality, can have a marked effect on the ligand's ICE and renal toxicity (Table 1 and Figure 4). Although the resulting DFT chelators were generally as effective in the rodents as their DADFT counterparts, they were less active in the primates. However, the tissue distribution of **6**, **8**, and **10** in rodents remains to be elucidated. Higher levels of these analogues in the critical target organs, that is, the liver, heart, and pancreas, could easily compensate for their somewhat lower ICE values. Nevertheless, at least one of the DFT polyethers (**8**) was sufficiently effective at iron clearance in rodents (ICE $11.7 \pm 1.2\%$)

and primates (ICE $18.0 \pm 5.2\%$) and had an acceptable toxicity profile to merit further studies.

EXPERIMENTAL SECTION

Materials. Reagents were purchased from Aldrich Chemical Co. (Milwaukee, WI). Compound **11** was obtained from Matrix Scientific (Columbia, SC). Fisher Optima grade solvents were routinely used. Reactions were run under a nitrogen atmosphere, and organic extracts were dried with sodium sulfate. Silica gel 40–63 from SiliCycle, Inc. (Quebec City, Quebec, Canada) was used for column chromatography. Melting points are uncorrected. Glassware that was presoaked in 3 N HCl for 15 min, washed with distilled water and distilled EtOH, and oven-dried, was used during the isolation of **6**, **8**, and **10**. Optical rotations were run at 589 nm (sodium D line) and 20 °C on a Perkin-Elmer 341 polarimeter, with c being concentration in grams of compound per 100 mL of solvent (CHCl₃, not indicated). ¹H NMR spectra were run in CDCl₃ (not indicated) at 400 MHz, and chemical shifts (δ) are given in parts per million downfield from tetramethylsilane. ¹³C NMR spectra were measured at 100 MHz, and chemical shifts (δ) are referenced to the residual solvent resonance of δ 77.16 for CDCl₃ (not indicated) or δ 39.52 for DMSO-*d*₆. Coupling constants (J) are in hertz. ESI-FTICR mass spectra are reported. The iron content of the Fe(III)–NTA solution was verified using a Perkin-Elmer 5100 PC Atomic Absorption Spectrophotometer (AAS). Data for the Job's plots were recorded on a UV-2550 UV–vis spectrophotometer.

Elemental analyses were performed by Atlantic Microlabs (Norcross, GA) and were within $\pm 0.4\%$ of the calculated values. Purity of the compounds is supported by high-pressure liquid chromatography (HPLC) ($\geq 95\%$ for **6**, **8**, and **10**) and by elemental analyses.

Male Sprague–Dawley rats were procured from Harlan Sprague–Dawley (Indianapolis, IN). Male *Cebus apella* monkeys (3.5–4 kg) were obtained from World Wide Primates (Miami, FL). Ultrapure salts were obtained from Johnson Matthey Electronics (Royston, United Kingdom). All hematological and biochemical studies were performed by Antech Diagnostics (Tampa, FL). Atomic absorption (AA) measurements were made on a Perkin-Elmer model 5100 PC (Norwalk, CT). A R-Rena-strip Lateral-flow Kit for the detection of Kim-1 in rat urine was obtained from BioAssay Works (Ijamsville, MD). A Chromatoreader ReaScan (Otsuka Electronics Co., Japan) was utilized to read the test strips and to allow for the quantitation of Kim-1 in rat urine.

Synthetic Methods. (S)-4,5-Dihydro-2-(3,5-dihydroxy-2-pyridinyl)-4-methyl-4-thiazolecarboxylic Acid (**6**). A solution of 50% (w/w) NaOH (13.7 g, 0.171 mol) in CH₃OH (135 mL) was added to **15** (4.85 g, 17.2 mmol) in CH₃OH (125 mL) over 13 min at 0 °C. The reaction mixture was warmed to rt over 19 h, and the bulk of the solvent was removed by rotary evaporation. The concentrate was treated with 3 M aqueous NaCl (150 mL) and was extracted with Et₂O (2 × 100 mL). The aqueous layer was cooled in ice, acidified with cold 6 N HCl (30 mL), and extracted with EtOAc (250 mL, 2 × 100 mL). The EtOAc extracts were washed with saturated NaCl (80 mL). Solvent was removed in vacuo, providing 4.18 g of **6** (96%) as an off white solid; mp 226–227 °C (dec); $[\alpha] +46.0^\circ$ (c 0.82, DMF). ¹H NMR (DMSO-*d*₆): δ 1.58 (s, 3 H), 3.27 (d, 1 H, $J = 11.3$), 3.69 (d, 1 H, $J = 11.7$), 6.72 (d, 1 H, $J = 2.4$), 7.80 (d, 1 H, $J = 2.0$), 10.82 (s, 1 H), 12.32 (s, 1 H), 13.20 (s, 1 H). ¹³C NMR (DMSO-*d*₆): δ 24.32, 38.48, 82.98, 108.59, 125.88, 131.13, 156.68, 157.58, 173.30, 173.74. HRMS m/z calcd for C₁₀H₁₁N₂O₄S, 255.0434 (M + H), 277.0253 (M + Na), 299.0073 (M – H + 2Na), 320.9892 (M – 2H + 3Na); found, 255.0439, 277.0255, 299.0077, 320.9899. Anal. (C₁₀H₁₀N₂O₄S) C, H, N.

(S)-4,5-Dihydro-2-[3-hydroxy-5-(3,6-dioxahexyloxy)-2-pyridinyl]-4-methyl-4-thiazolecarboxylic Acid (**8**). A solution of 50% (w/w) NaOH (1.46 mL, 47.0 mmol) in CH₃OH (40 mL) was added dropwise to a solution of **17** (1.66 g, 4.32 mmol) in CH₃OH (20 mL) at 0 °C. The reaction mixture was stirred at rt for 6 h, and the bulk of the solvent was removed under reduced pressure. The residue was treated with 3 M aqueous NaCl (50 mL) and was extracted with Et₂O (2 × 30 mL). The aqueous layer was cooled in ice, acidified with 2 N HCl to pH 2, and extracted with EtOAc (5 × 40 mL). Combined EtOAc layers were washed with saturated NaCl (60 mL). Solvent removal in vacuo

furnished 1.49 g of **8** (97%) as a yellow oil: $[\alpha] +25.3^\circ$ (c 0.88). ¹H NMR: δ 1.73 (s, 3 H), 3.22 (d, 1 H, $J = 12.0$), 3.41 (s, 3 H), 3.59–3.61 (m, 2 H), 3.72–3.74 (m, 2 H), 3.83 (d, 1 H, $J = 11.6$), 3.88 (t, 2 H, $J = 4.8$), 4.19 (t, 2 H, $J = 4.4$), 6.84 (d, 1 H, $J = 2.4$), 7.94 (d, 1 H, $J = 2.4$). ¹³C NMR: δ 24.62, 39.13, 58.98, 67.99, 69.28, 70.63, 71.81, 82.83, 107.67, 126.98, 131.64, 158.15, 158.44, 174.59, 175.94. HRMS m/z calcd for C₁₅H₂₁N₂O₆S, 357.1115 (M + H); found, 357.1125. Anal. (C₁₅H₂₀N₂O₆S) C, H, N.

(S)-4,5-Dihydro-2-[3-hydroxy-4-(3,6-dioxahexyloxy)-2-pyridinyl]-4-methyl-4-thiazolecarboxylic Acid (**10**). Compound **14** (0.78 g, 4.58 mmol), pH 6 phosphate buffer (30 mL), and NaHCO₃ (0.44 g, 5.23 mmol) were successively added to a solution of **24** (0.78 g, 3.27 mmol) in degassed CH₃OH (30 mL). The reaction mixture was heated at 75 °C for 48 h with stirring, cooled, and concentrated by rotary evaporation. The residue was dissolved in distilled H₂O (25 mL), and the aqueous layer was acidified with cold 2 N HCl to pH <2 followed by extraction with EtOAc (5 × 50 mL). Concentration in vacuo resulted in 1.15 g of **10** (95%) as a light yellow oil: $[\alpha] +52.8^\circ$ (c 0.40). ¹H NMR: δ 1.73 (s, 3 H), 3.24 (d, 1 H, $J = 11.6$), 3.39 (s, 3 H), 3.56–3.58 (m, 2 H), 3.73–3.75 (m, 2 H), 3.85 (d, 1 H, $J = 11.6$), 3.94 (t, 2 H, $J = 4.8$), 4.27 (t, 2 H, $J = 4.8$), 6.88 (d, 1 H, $J = 5.2$), 8.08 (d, 1 H, $J = 4.8$). ¹³C NMR: δ 24.65, 39.52, 59.08, 68.57, 69.31, 70.87, 71.94, 83.67, 109.81, 133.20, 141.56, 147.16, 154.39, 175.11, 176.26. HRMS m/z calcd for C₁₅H₂₁N₂O₆S, 357.1115 (M + H); found, 357.1115. Anal. (C₁₅H₂₀N₂O₆S) C, H, N.

3,5-Bis(4-methoxybenzyloxy)pyridine-2-carbonitrile (**12**). Sodium hydride (60%, 3.66 g, 91.5 mmol) was added to 4-methoxybenzyl alcohol (11.5 mL, 92.6 mmol) in DMF (89 mL). The reaction mixture was stirred for 50 min and was cooled in an ice water bath, followed by addition of **11** (5.13 g, 36.6 mmol). After it was stirred at rt for 30 min and heated at 95–100 °C for 18 h, the reaction was quenched at 0 °C with EtOH and was concentrated by rotary evaporation under high vacuum. The residue was treated with H₂O (250 mL) and extracted with warm EtOAc (400 mL, 2 × 100 mL). The organic extracts were washed with saturated NaCl (150 mL). Purification by flash column chromatography using 2% acetone/CH₂Cl₂ gave 10.11 g of **12** (73%) as a white solid; mp 122–122.5 °C. ¹H NMR: δ 3.82 (s, 3 H), 3.83 (s, 3 H), 5.04 (s, 2 H), 5.11 (s, 2 H), 6.85 (d, 1 H, $J = 2.0$), 6.92 (dd, 4 H, $J = 8.6, 6.6$), 7.31 (t, 4 H, $J = 8.6$), 8.01 (d, 1 H, $J = 2.0$). ¹³C NMR: δ 55.45, 55.47, 70.98, 71.00, 106.86, 114.41, 115.63, 116.26, 126.83, 126.94, 129.04, 129.56, 131.98, 158.41, 159.10, 160.00, 160.14. HRMS m/z calcd for C₂₂H₂₁N₂O₄, 377.1496 (M + H); found, 377.1500. Anal. (C₂₂H₂₀N₂O₄) C, H, N.

3,5-Dihydroxy-2-pyridinecarbonitrile (**13**). TFA (477 g) was added over 26 min to **12** (9.63 g, 25.6 mmol) and pentamethylbenzene (38.2 g, 0.258 mol) with ice bath cooling. The reaction mixture was stirred at rt for 22 h, and volatiles were removed by rotary evaporation. The residue was partitioned between cold 2 N NaOH (180 mL) and Et₂O (350 mL) and separated. The Et₂O layer was back extracted with 0.5 N NaOH (80 mL). The combined aqueous phase was extracted with Et₂O (100 mL), cooled in an ice water bath, and combined with cold 2 M HCl (220 mL) and saturated NaCl (100 mL). The aqueous layer was extracted with EtOAc (250 mL, 2 × 120 mL). The latter organic extracts were washed with saturated NaCl (150 mL) and concentrated in vacuo, giving 3.70 g of **13** (quantitative) as a light tan solid. ¹H NMR (DMSO-*d*₆): δ 6.80 (d, 1 H, $J = 2.4$), 7.74 (d, 1 H, $J = 2.0$), 10.98 (s, 1 H), 11.39 (s, 1 H). ¹³C NMR (DMSO-*d*₆): δ 108.69, 111.17, 116.74, 132.54, 158.10, 159.21. HRMS m/z calcd for C₆H₃N₂O₂, 135.0200 (M – H); found, 135.0196. An analytical sample was recrystallized from aqueous EtOH. At > 300 °C, the sample was dark but not melted. Anal. (C₆H₃N₂O₂) C, H, N.

Ethyl (S)-4,5-Dihydro-2-(3,5-dihydroxy-2-pyridinyl)-4-methyl-4-thiazolecarboxylate (**15**). A degassed solution of 0.1 M phosphate buffer (pH 6, 310 mL) and CH₃OH (300 mL) was added to **13** (4.04 g, 29.7 mmol) and **14** (6.95 g, 40.5 mmol). The pH of the reaction solution was adjusted to 6.0 with NaHCO₃ (4.92 g, 58.6 mmol). The reaction mixture was heated at 73–76 °C for 45 h with stirring, cooled to 0 °C, and reduced in volume by rotary evaporation. The residue was acidified to pH ~ 1 with cold 2 N HCl (61 mL) followed by extraction with EtOAc (300 mL, 2 × 100 mL). The organic layer was washed with saturated NaCl (100 mL), concentrated in vacuo, and dried with toluene, resulting in 6.30 g of **6**. Iodoethane (3.0 mL, 37.5 mmol) and

DIEA (6.5 mL, 37.3 mmol) were successively added to **6** in DMF (130 mL), and the solution was stirred at rt for 47 h. After solvent removal under high vacuum, the residue was treated with 12:5 0.5 M HCl/saturated NaCl (170 mL) followed by extraction with EtOAc (150 mL, 4 × 70 mL). The EtOAc layers were washed with 100 mL portions of 1% NaHSO₃ and saturated NaCl, and the solvent was evaporated. Purification by column chromatography using (5% acetone/CH₂Cl₂) gave 5.88 g of **15** (70%) as a pale yellow solid; mp 85–87.5 °C, [α] +35.6° (c 0.74). ¹H NMR: δ 1.32 (t, 3 H, *J* = 7.2), 1.69 (s, 3 H), 3.20 (d, 1 H, *J* = 11.7), 3.79 (d, 1 H, *J* = 11.7), 4.27 (q, 2 H, *J* = 7.2), 6.77 (d, 1 H, *J* = 2.4), 7.82 (d, 1 H, *J* = 2.3). ¹³C NMR: δ 14.23, 24.78, 39.60, 62.33, 83.67, 110.11, 127.71, 130.80, 156.17, 157.79, 173.21, 174.02. HRMS *m/z* calcd for C₁₂H₁₅N₂O₄S, 283.0747 (M + H), 305.0567 (M + Na); found, 283.0751, 305.0573. Anal. (C₁₂H₁₄N₂O₄S) C, H, N.

Ethyl (S)-4,5-Dihydro-2-[3-hydroxy-5-(3,6-dioxahexyloxy)-2-pyridinyl]-4-methyl-4-thiazolecarboxylate (17). Flame-activated K₂CO₃ (0.72 g, 5.21 mmol) was added to a mixture of **16** (0.96 g, 3.2 mmol) and **15** (0.90 g, 3.19 mmol) in dry acetone (25 mL). The reaction mixture was heated at reflux for 24 h. After it was cooled to rt, the solvent was removed by rotary evaporation. The residue was treated with 1:9 0.2 N HCl/saturated NaCl (50 mL) and was extracted with EtOAc (4 × 30 mL). The organic extracts were washed with saturated NaCl (50 mL), and solvent was removed in vacuo. Column chromatography using 1:2:7 CH₃OH/hexane/CH₂Cl₂ furnished 0.80 g of **17** (65%) as a viscous oil; [α] +30.9° (c 1.12). ¹H NMR: δ 1.30 (t, 3 H, *J* = 7.0), 1.67 (s, 3 H), 3.19 (d, 1 H, *J* = 11.3), 3.40 (s, 3 H), 3.56–3.62 (m, 2 H), 3.70–3.75 (m, 2 H), 3.80 (d, 1 H, *J* = 11.7), 3.86–3.93 (m, 2 H), 4.19 (t, 2 H, *J* = 4.7), 4.25 (q, 2 H, *J* = 7.0), 6.80 (d, 1 H, *J* = 2.3), 7.95 (d, 1 H, *J* = 2.3), 12.37 (s, 1 H). ¹³C NMR: δ 14.23, 24.77, 39.45, 59.25, 62.04, 68.11, 69.46, 70.99, 72.01, 83.84, 107.63, 127.72, 131.49, 157.39, 158.22, 172.87, 173.96. HRMS *m/z* calcd for C₁₇H₂₅N₂O₆S, 385.1428 (M + H), 407.1247 (M + Na); found, 385.1432, 407.1266. Anal. (C₁₇H₂₄N₂O₆S) C, H, N.

2-Methyl-3-(benzyloxy)-4-(3,6-dioxahexyloxy)pyridine (19). Flame-activated K₂CO₃ (27.6 g, 0.20 mol) and **16** (27.4 g, 0.10 mol) were added to **18** (21.5 g, 0.10 mol) in dry CH₃CN (500 mL). The reaction mixture was heated at reflux for 24 h. After it was cooled to rt, the solvent was evaporated by rotary evaporation. The residue was treated with 1.7 M aqueous NaCl (200 mL) and was extracted with CH₂Cl₂ (4 × 150 mL). The organic extracts were washed with saturated NaCl (300 mL). After the solvent was removed in vacuo, column chromatography using 4:4:2 EtOAc/petroleum ether/acetone furnished 21.5 g of **19** (68%) as a colorless viscous oil. ¹H NMR: δ 2.42 (s, 3 H), 3.34 (s, 3 H), 3.51–3.53 (m, 2 H), 3.69–3.71 (m, 2 H), 3.91 (t, 2 H, *J* = 4.8), 4.24 (t, 2 H, *J* = 4.4), 5.02 (s, 2 H), 6.72 (d, 1 H, *J* = 5.6), 7.31–7.40 (m, 3 H), 7.44–7.49 (m, 2 H), 8.12 (d, 1 H, *J* = 5.6). ¹³C NMR: δ 19.34, 59.16, 67.86, 69.45, 70.92, 71.99, 74.57, 106.68, 128.21, 128.45, 128.49, 137.53, 142.32, 145.41, 153.40, 157.64. HRMS *m/z* calcd for C₁₈H₂₄NO₄, 318.1700 (M + H); found, 318.1714. Anal. (C₁₈H₂₃NO₄·0.2H₂O) C, H, N.

4-(3,6-Dioxahexyloxy)-3-(benzyloxy)-2-pyridinemethanol (20). An ice-cooled solution of *m*-CPBA (3.67 g, 36.0 mmol) in CH₂Cl₂ (75 mL) was added slowly to **19** (10.4 g, 32.8 mmol) in CH₂Cl₂ (50 mL) over 15 min at 0 °C. The reaction mixture was warmed to rt, stirred for 6 h, and diluted with CH₂Cl₂ (150 mL). The reaction mixture was washed with 5% Na₂CO₃ (3 × 100 mL) and saturated NaCl (100 mL) and was concentrated under reduced pressure to give a colorless oil. Acetic anhydride (80 mL, 0.85 mol) was added, and the reaction mixture was heated at 130 °C for 2 h. The solvent was removed under reduced pressure, and the residue was dissolved in H₂O (100 mL). The pH of the aqueous solution was adjusted to 8 with 2 N NaOH, and the aqueous solution was extracted with CH₂Cl₂ (3 × 100 mL). The organic fractions were combined and washed with saturated NaCl (100 mL) and concentrated in vacuo. The residue was dissolved in CH₃OH, treated with decolorizing charcoal, filtered, and concentrated to yield a brown oil, which was dissolved in EtOH (40 mL). Aqueous 1 M NaOH (80 mL) was added, and the reaction mixture was refluxed for 4 h and cooled. Extraction with CH₂Cl₂ (4 × 100 mL), washing with saturated NaCl (100 mL), concentration under reduced pressure, and column chromatography using 10% CH₃OH/CHCl₃ provided 9.52 g (87%) of

20 as a light brown oil. ¹H NMR: δ 3.34 (s, 3 H), 3.52–3.54 (m, 2 H), 3.69–3.71 (m, 2 H), 3.92 (t, 2 H, *J* = 5.2), 4.28 (t, 2 H, *J* = 4.4), 4.65 (s, 2 H), 5.09 (s, 2 H), 6.83 (d, 1 H, *J* = 5.2), 7.32–7.39 (m, 3 H), 7.40–7.44 (m, 2 H), 8.19 (d, 1 H, *J* = 5.6). ¹³C NMR: δ 59.20, 60.23, 68.13, 69.44, 70.96, 72.04, 74.79, 107.83, 128.49, 128.54, 128.63, 137.15, 140.53, 144.66, 152.98, 157.52. HRMS *m/z* calcd for C₁₈H₂₄NO₅, 334.1649 (M + H), 356.1468 (M + Na); found, 334.1648, 356.1455. Anal. (C₁₈H₂₃NO₅) C, H, N.

4-(3,6-Dioxahexyloxy)-3-(benzyloxy)pyridine-2-carboxaldehyde (21). Triethylamine (70 mL, 0.29 mol) followed by DMSO (70 mL) was added to **20** (16.5 g, 49.0 mmol) in CHCl₃ (100 mL). Sulfur trioxide–pyridine complex (35 g, 0.22 mol) was slowly added over 35 min to the reaction mixture with ice bath cooling. After it was warmed to rt, the reaction mixture was stirred overnight and was diluted with CHCl₃ (200 mL). The organic phase was washed with H₂O (3 × 200 mL) and saturated NaCl (100 mL). After the solvent was removed in vacuo, column chromatography using 5:5:1 EtOAc/CHCl₃/CH₃OH furnished 13.61 g of **21** (83%) as a viscous colorless oil. ¹H NMR: δ 3.34 (s, 3 H), 3.52–3.54 (m, 2 H), 3.70–3.72 (m, 2 H), 3.95 (t, 2 H, *J* = 4.4), 4.30 (t, 2 H, *J* = 4.4), 5.24 (s, 2 H), 7.02 (d, 1 H, *J* = 5.2), 7.32–7.39 (m, 3 H), 7.41–7.46 (m, 2 H), 8.39 (d, 1 H, *J* = 5.6), 10.25 (s, 1 H). ¹³C NMR: δ 59.17, 68.54, 69.23, 70.94, 71.97, 76.24, 111.69, 128.68, 128.75, 128.87, 136.16, 145.87, 146.90, 148.14, 159.49, 189.87. HRMS *m/z* calcd for C₁₈H₂₁NNaO₅, 354.1312 (M + Na); found, 354.1326. Anal. (C₁₈H₂₁NO₅) C, H, N.

4-(3,6-Dioxahexyloxy)-3-(benzyloxy)pyridine-2-carboxaldehyde Oxime (22). Hydroxylamine hydrochloride (4.2 g, 60.0 mmol) and NaOAc (5.2 g, 60.0 mmol) were added to a solution of **21** (13.5 g, 40.7 mmol) in CH₃OH (50 mL), and the reaction mixture was heated at reflux for 2 h. The reaction mixture was concentrated by rotary evaporation, and the residue was treated with saturated NaCl (100 mL) and 0.1 M aqueous citric acid (100 mL) and then was extracted with EtOAc (2 × 100 mL). The organic layers were washed with H₂O (100 mL) and saturated NaCl (100 mL). The solvent was removed in vacuo, providing 12.7 g (90%) of **22** as a pale solid; mp 72–73 °C. ¹H NMR: δ 3.34 (s, 3 H), 3.46–3.51 (m, 2 H), 3.64–3.71 (m, 2 H), 3.92 (t, 2 H, *J* = 4.4), 4.27 (t, 2 H, *J* = 4.4), 5.10 (s, 2 H), 6.85 (d, 1 H, *J* = 5.6), 7.29–7.46 (m, 5 H), 8.28 (d, 1 H, *J* = 5.2), 8.46 (s, 1 H). ¹³C NMR: δ 59.14, 68.12, 69.28, 70.86, 71.94, 75.67, 108.62, 128.42, 128.55, 128.59, 136.70, 143.43, 144.81, 145.23, 146.71, 158.66. HRMS *m/z* calcd for C₁₈H₂₁N₂O₅, 345.1450 (M – H); found, 345.1426. Anal. (C₁₈H₂₂NO₅) C, H, N.

4-(3,6-Dioxahexyloxy)-3-(benzyloxy)pyridine-2-carbonitrile (23). Compound **22** (12.15 g, 36.71 mmol) was dissolved in Ac₂O (40 mL) and heated at reflux for 8 h under a Drierite tube. The reaction mixture was concentrated by rotary evaporation and was dissolved in 8% aqueous NaHCO₃ (100 mL) and extracted with CHCl₃ (100 mL, 2 × 50 mL). Combined organic fractions were washed with 4% NaHCO₃ (50 mL) and saturated NaCl (100 mL) followed by solvent removal in vacuo. Purification by flash chromatography eluting with 10% CH₃OH/CH₂Cl₂ gave 11.31 g (94%) of **23** as a pale solid; mp 34–35 °C. ¹H NMR: δ 3.34 (s, 3 H), 3.53–3.55 (m, 2 H), 3.70–3.72 (m, 2 H), 3.93 (t, 2 H, *J* = 4.8), 4.27 (t, 2 H, *J* = 4.4), 5.31 (s, 2 H), 6.98 (d, 1 H, *J* = 5.6), 7.31–7.38 (m, 3 H), 7.49–7.52 (m, 2 H), 8.21 (d, 1 H, *J* = 5.2). ¹³C NMR: δ 59.14, 68.59, 69.09, 70.92, 71.94, 75.84, 111.27, 115.43, 128.60, 128.66, 128.73, 128.84, 135.78, 147.21, 148.28, 158.42. HRMS *m/z* calcd for C₁₈H₂₀N₂NaO₄, 351.1315 (M + Na); found, 351.1325. Anal. (C₁₈H₂₀N₂O₄) C, H, N.

4-(3,6-Dioxahexyloxy)-3-hydroxy-2-pyridinecarbonitrile (24). Palladium on carbon (10%, 0.065 g) was added to a solution of **23** (1.30 g, 3.95 mmol) in CH₃OH (15 mL), and the mixture was stirred under H₂ at 1 atm for 2 h. The reaction mixture was filtered through Celite, and the solids were washed with CH₃OH (3 × 5 mL). The filtrate was concentrated under reduced pressure, and the residue was subjected to column chromatography eluting with 10% CH₃OH/EtOAc, furnishing 0.80 g (85%) of **24** as a colorless oil. ¹H NMR: δ 3.42 (s, 3 H), 3.61–3.63 (m, 2 H), 3.75–3.77 (m, 2 H), 3.92 (t, 2 H, *J* = 4.8), 4.24 (t, 2 H, *J* = 4.4), 6.91 (d, 1 H, *J* = 4.8), 8.10 (d, 1 H, *J* = 5.6). ¹³C NMR: δ 58.92, 68.66, 69.05, 70.52, 71.78, 110.68, 115.28, 120.29, 143.49, 148.84,

153.72. HRMS m/z calcd for $C_{11}H_{14}N_2NaO_4$, 261.0846 ($M + Na$); found, 261.0849. Anal. ($C_{11}H_{14}N_2O_4$) C, H, N.

Job's Plots for 6, 8, and 10. The stoichiometries of the ligand–Fe(III) complexes of **6**, **8**, and **10** were determined spectrophotometrically using Job's plots. Solutions were monitored at the visible λ_{max} of the Fe(III) complexes (498 nm for **6**, 484 nm for **8**, and 485 nm for **10**). A 100 mM Tris HCl buffer was used to maintain the pH at 7.4. Solutions containing different ligand/Fe(III) ratios were prepared by mixing appropriate volumes of 1.0 mM ligand solution and 1.0 mM Fe(III)–nitriloacetate (NTA) in Tris-HCl buffer. The 1.0 mM Fe(III)–NTA solution was prepared immediately prior to use by dilution of a 41.6 mM Fe(III)–NTA stock solution with the Tris HCl buffer, whereas the ligand's stock solution was prepared by dissolving the ligand as its monosodium salt in Tris HCl buffer at pH 7.4. The Fe(III)–NTA stock solution was prepared by mixing equal volumes of 90 mM of $FeCl_3$ and 180 mM trisodium NTA. The iron content of the Fe(III)–NTA solution was verified by AAS.

Biological Methods. All animal experimental treatment protocols were reviewed and approved by the University of Florida's Institutional Animal Care and Use Committee.

Cannulation of Bile Duct in Noniron-Overloaded Rats. The cannulation has been described previously.^{37,48} Bile samples were collected from male Sprague–Dawley rats (400–450 g) at 3 h intervals for up to 48 h. The urine sample(s) was taken at 24 h intervals. Sample collection and handling are as previously described.^{37,48}

Iron Loading of *C. apella* Monkeys. The monkeys were iron overloaded with intravenous iron dextran as specified in earlier publications^{48,71} to provide about 500 mg of iron per kg of body weight; the serum transferrin iron saturation rose to between 70 and 80%. At least 20 half-lives, 60 days,⁷² elapsed before any of the animals were used in experiments evaluating iron-chelating agents.

Primate Fecal and Urine Samples. Fecal and urine samples were collected at 24 h intervals and processed as described previously.^{37,48,73} Briefly, the collections began 4 days prior to the administration of the test drug and continued for an additional 5 days after the drug was given. Iron concentrations were determined by flame absorption spectroscopy as presented in other publications.^{48,74}

Drug Preparation and Administration: Iron Clearance. In the iron-clearing experiments, the rats were given **6**, **8**, and **10** po at a dose of 300 $\mu\text{mol/kg}$. The primates were given **6**, **8**, and **10** po at a dose of 75 $\mu\text{mol/kg}$; ligand **10** was also given sc at a dose of 75 $\mu\text{mol/kg}$. The drugs were administered to the rats and primates as their monosodium salts (prepared by the addition of 1 equiv of NaOH to a suspension of the free acid in distilled water). Drug preparation for the rodent urinary Kim-1 excretion studies involving **1**, **6**, **8**, and **10** are described below.

Calculation of Iron Chelator Efficiency. In the text below, the term "ICE" is used as a measure of the amount of iron excretion induced by a chelator. The ICE, expressed as a percent, is calculated as (ligand-induced iron excretion/theoretical iron excretion) \times 100. To illustrate, the theoretical iron excretion after administration of 1 mmol of DFO, a hexadentate chelator that forms a 1:1 complex with Fe(III), is 1 milligram of iron. Two millimoles of DFT (**1**, Table 1), a tridentate iron chelator that forms a 2:1 complex with Fe(III), is required for the theoretical excretion of 1 milligram of iron. The theoretical iron outputs of the chelators were generated on the basis of a 2:1 ligand:iron complex. The efficiencies in the rats and monkeys were calculated as set forth elsewhere.^{38,73} Data are presented as the mean \pm the standard error of the mean; p values were generated via a one-tailed Student's t test in which the inequality of variances was assumed, and a p value of <0.05 was considered significant.

Drug Preparation and Administration: Rodent Toxicity/Urinary Kim-1 Excretion Studies. The impact of ligands **1**, **6**, **8**, and **10** on urinary Kim-1 excretion was evaluated in rodents. The chelators were administered to the rats po as their monosodium salts, prepared as described above, twice daily at a dose of 237 $\mu\text{mol/kg/dose}$ (474 $\mu\text{mol/kg/day}$) for up to 7 days. The studies were performed on rats with normal iron stores. The rats were fasted overnight and were given the first dose of the chelator first thing in the morning. The rats were fed ~ 3 h postdrug and had access to food for ~ 5 h before being fasted overnight.

Collection of Urine for Kim-1 Studies. The rats were housed in individual metabolic cages. Urine samples were collected from the metabolic cages at 24 h intervals. A baseline (day 0) urine sample was collected and assessed for its Kim-1 content; each animal served as its own control. The urine was collected chilled as previously described.⁵⁵

Performance of Urinary Kim-1 Studies. The chilled urine was collected, vortexed, and warmed to room temperature; any sediment in the samples was allowed to settle. The Kim-1 content was assessed using a Rat Kim-1 Rapid Test Kit according to the manufacturer's instructions. The result was read using a ReaScan Test Reader. The quantity of Kim-1 excreted in the urine per day was calculated by multiplying the concentration of Kim-1 (ng/mL urine) \times 24 h urine volume, divided by the weight of the animal. The result is expressed as urinary Kim-1 (ng/kg/24 h). Data are presented as the mean \pm the standard error of the mean; p values were generated via a one-tailed Student's t test in which the inequality of variances was assumed, and a p value of <0.05 was considered significant.

■ ASSOCIATED CONTENT

📄 Supporting Information

Elemental analytical data for synthesized compounds. This material is available free of charge via the Internet at <http://pubs.acs.org>.

■ AUTHOR INFORMATION

✉ Corresponding Author

*Tel: 352-273-7725. Fax: 352-392-8406. E-mail: rayb@ufl.edu.

Notes

The authors declare the following competing financial interest(s): Patents filed.

■ ACKNOWLEDGMENTS

The project described was supported by grant number R37DK049108 from the National Institutes of Health. The content is solely the responsibility of the authors and does not necessarily represent the official views of the National Institute of Diabetes and Digestive and Kidney Diseases or the National Institutes of Health. We thank Elizabeth M. Nelson and Katie Ratliff-Thompson for their technical assistance and Miranda E. Coger for her editorial and organizational support. We acknowledge the spectroscopy services in the Chemistry Department, University of Florida, for the mass spectrometry analyses.

■ ABBREVIATIONS USED

DFO, desferrioxamine B mesylate; DFT, desferrithiocin, (S)-4,5-dihydro-2-(3-hydroxy-2-pyridinyl)-4-methyl-4-thiazolecarboxylic acid; ICE, iron-clearing efficiency; DADFT, desazadesferri-thiocin; SAR, structure–activity relationship; BUN, blood urea nitrogen; SCr, serum creatinine; PR, performance ratio; Kim-1, kidney injury molecule-1; MIC, maximum iron clearance; b.i.d., twice daily

■ REFERENCES

- (1) Raymond, K. N.; Carrano, C. J. Coordination Chemistry and Microbial Iron Transport. *Acc. Chem. Res.* **1979**, *12*, 183–190.
- (2) Byers, B. R.; Arceneaux, J. E. Microbial Iron Transport: Iron Acquisition by Pathogenic Microorganisms. *Met. Ions Biol. Syst.* **1998**, *35*, 37–66.
- (3) Bergeron, R. J. Iron: A Controlling Micronutrient in Proliferative Processes. *Trends Biochem. Sci.* **1986**, *11*, 133–136.
- (4) Theil, E. C.; Huynh, B. H. Ferritin Mineralization: Ferroxidation and Beyond. *J. Inorg. Biochem.* **1997**, *67*, 30.

- (5) Ponka, P.; Beaumont, C.; Richardson, D. R. Function and Regulation of Transferrin and Ferritin. *Semin. Hematol.* **1998**, *35*, 35–54.
- (6) Brittenham, G. M. Disorders of Iron Metabolism: Iron Deficiency and Overload. In *Hematology: Basic Principles and Practice*, 3rd ed.; Hoffman, R., Benz, E. J., Shattil, S. J., Furie, B., Cohen, H. J., et al., Eds.; Churchill Livingstone: New York, 2000; pp 397–428.
- (7) Olivieri, N. F.; Brittenham, G. M. Iron-Chelating Therapy and the Treatment of Thalassemia. *Blood* **1997**, *89*, 739–761.
- (8) Vichinsky, E. P. Current Issues with Blood Transfusions in Sickle Cell Disease. *Semin. Hematol.* **2001**, *38*, 14–22.
- (9) Kersten, M. J.; Lange, R.; Smeets, M. E.; Vreugdenhil, G.; Roozendaal, K. J.; Lameijer, W.; Goudsmit, R. Long-Term Treatment of Transfusional Iron Overload with the Oral Iron Chelator Deferiprone (L1): A Dutch Multicenter Trial. *Ann. Hematol.* **1996**, *73*, 247–252.
- (10) Conrad, M. E.; Umbreit, J. N.; Moore, E. G. Iron Absorption and Transport. *Am. J. Med. Sci.* **1999**, *318*, 213–229.
- (11) Lieu, P. T.; Heiskala, M.; Peterson, P. A.; Yang, Y. The Roles of Iron in Health and Disease. *Mol. Aspects Med.* **2001**, *22*, 1–87.
- (12) Graf, E.; Mahoney, J. R.; Bryant, R. G.; Eaton, J. W. Iron-Catalyzed Hydroxyl Radical Formation. Stringent Requirement for Free Iron Coordination Site. *J. Biol. Chem.* **1984**, *259*, 3620–3624.
- (13) Halliwell, B. Iron, Oxidative Damage, and Chelating Agents. In *The Development of Iron Chelators for Clinical Use*; Bergeron, R. J., Brittenham, G. M., Eds.; CRC: Boca Raton, FL, 1994; pp 33–56.
- (14) Koppenol, W. Kinetics and Mechanism of the Fenton Reaction: Implications for Iron Toxicity. In *Iron Chelators: New Development Strategies*; Badman, D. G., Bergeron, R. J., Brittenham, G. M., Eds.; Saratoga: Ponte Vedra Beach, FL, 2000; pp 3–10.
- (15) Hazen, S. L.; d'Avignon, A.; Anderson, M. M.; Hsu, F. F.; Heáinecke, J. W. Human Neutrophils Employ the Myeloperoxidase-Hydrogen Peroxide-Chloride System to Oxidize α -Amino Acids to a Family of Reactive Aldehydes. Mechanistic Studies Identifying Labile Intermediates along the Reaction Pathway. *J. Biol. Chem.* **1998**, *273*, 4997–5005.
- (16) Millán, M.; Sobrino, T.; Arenillas, J. F.; Rodríguez-Yáñez, M.; García, M.; Nombela, F.; Castellanos, M.; de la Ossa, N. P.; Cuadras, P.; Serena, J.; Castillo, J.; Dávalos, A. Biological Signatures of Brain Damage Associated with High Serum Ferritin Levels in Patients with Acute Ischemic Stroke and Thrombolytic Treatment. *Dis. Markers* **2008**, *25*, 181–188.
- (17) Zecca, L.; Casella, L.; Albertini, A.; Bellei, C.; Zucca, F. A.; Engelen, M.; Zadlo, A.; Szweczyk, G.; Zareba, M.; Sarna, T. Neuromelanin Can Protect Against Iron-Mediated Oxidative Damage in System Modeling Iron Overload of Brain Aging and Parkinson's Disease. *J. Neurochem.* **2008**, *106*, 1866–1875.
- (18) Pietrangelo, A. Iron Chelation Beyond Transfusion Iron Overload. *Am. J. Hematol.* **2007**, *82*, 1142–1146.
- (19) Dunaief, J. L. Iron Induced Oxidative Damage as a Potential Factor in Age-Related Macular Degeneration: The Cogan Lecture. *Invest. Ophthalmol. Vis. Sci.* **2006**, *47*, 4660–4664.
- (20) Hua, Y.; Nakamura, T.; Keep, R. F.; Wu, J.; Schallert, T.; Hoff, J. T.; Xi, G. Long-Term Effects of Experimental Intracerebral Hemorrhage: The Role of Iron. *J. Neurosurg.* **2006**, *104*, 305–312.
- (21) Pippard, M. J. Iron Overload and Iron Chelation Therapy in Thalassemia and Sickle Cell Haemoglobinopathies. *Acta Haematol.* **1987**, *78*, 206–211.
- (22) Olivieri, N. F. Progression of Iron Overload in Sickle Cell Disease. *Semin. Hematol.* **2001**, *38*, 57–62.
- (23) Malcovati, L. Impact of Transfusion Dependency and Secondary Iron Overload on the Survival of Patients with Myelodysplastic Syndromes. *Leuk. Res.* **2007**, *31*, S2–S6.
- (24) Kalinowski, D. S.; Richardson, D. R. The Evolution of Iron Chelators for the Treatment of Iron Overload Disease and Cancer. *Pharm. Rev.* **2005**, *57*, 547–583.
- (25) Brittenham, G. M. Iron-Chelating Therapy for Transfusional Iron Overload. *N. Engl. J. Med.* **2011**, *364*, 146–156.
- (26) *Desferal*; Novartis Pharmaceuticals Corporation: East Hanover, NJ, 2008; <http://www.pharma.us.novartis.com/product/pi/pdf/desferal.pdf>.
- (27) Hoffbrand, A. V.; Al-Refaie, F.; Davis, B.; Siritanakatkul, N.; Jackson, B. F. A.; Cochrane, J.; Prescott, E.; Wonke, B. Long-Term Trial of Deferiprone in 51 Transfusion-Dependent Iron Overloaded Patients. *Blood* **1998**, *91*, 295–300.
- (28) Olivieri, N. F. Long-Term Therapy with Deferiprone. *Acta Haematol.* **1996**, *95*, 37–48.
- (29) Olivieri, N. F.; Brittenham, G. M.; McLaren, C. E.; Templeton, D. M.; Cameron, R. G.; McClelland, R. A.; Burt, A. D.; Fleming, K. A. Long-Term Safety and Effectiveness of Iron-Chelation Therapy with Deferiprone from Thalassemia Major. *N. Engl. J. Med.* **1998**, *339*, 417–423.
- (30) Richardson, D. R. The Controversial Role of Deferiprone in the Treatment of Thalassemia. *J. Lab. Clin. Med.* **2001**, *137*, 324–329.
- (31) Nisbet-Brown, E.; Olivieri, N. F.; Giardini, P. J.; Grady, R. W.; Neufeld, E. J.; Séchaud, R.; Krebs-Brown, A. J.; Anderson, J. R.; Alberti, D.; Sizer, K. C.; Nathan, D. G. Effectiveness and Safety of ICL670 in Iron-Loaded Patients with Thalassemia: A Randomised, Double-Blind, Placebo-Controlled, Dose-Escalation Trial. *Lancet* **2003**, *361*, 1597–1602.
- (32) Galanello, R.; Piga, A.; Alberti, D.; Rouan, M.-C.; Bigler, H.; Séchaud, R. Safety, Tolerability, and Pharmacokinetics of ICL670, a New Orally Active Iron-Chelating Agent in Patients with Transfusion-Dependent Iron Overload Due to β -Thalassemia. *J. Clin. Pharmacol.* **2003**, *43*, 565–572.
- (33) Cappellini, M. D. Iron-Chelating Therapy with the New Oral Agent ICL670 (Exjade). *Best Pract. Res. Clin. Haematol.* **2005**, *18*, 289–298.
- (34) *Exjade Prescribing Information*; Novartis Pharmaceuticals Corporation: East Hanover, NJ, March, 2012; <http://www.pharma.us.novartis.com/product/pi/pdf/exjade.pdf>.
- (35) Pippard, M. J. Desferrioxamine-Induced Iron Excretion in Humans. *Bailliere's Clin. Haematol.* **1989**, *2*, 323–343.
- (36) Giardina, P. J.; Grady, R. W. Chelation Therapy in β -Thalassemia: An Optimistic Update. *Semin. Hematol.* **2001**, *38*, 360–366.
- (37) Bergeron, R. J.; Streiff, R. R.; Creary, E. A.; Daniels, R. D., Jr.; King, W.; Luchetta, G.; Wiegand, J.; Moerker, T.; Peter, H. H. A Comparative Study of the Iron-Clearing Properties of Desferrioxamine Analogues with Desferrioxamine B in a *Cebus* Monkey Model. *Blood* **1993**, *81*, 2166–2173.
- (38) Bergeron, R. J.; Wiegand, J.; McManis, J. S.; McCosar, B. H.; Weimar, W. R.; Brittenham, G. M.; Smith, R. E. Effects of C-4 Stereochemistry and C-4' Hydroxylation on the Iron Clearing Efficiency and Toxicity of Desferrioxamine Analogues. *J. Med. Chem.* **1999**, *42*, 2432–2440.
- (39) Bergeron, R. J.; Wiegand, J.; McManis, J. S.; Bussenius, J.; Smith, R. E.; Weimar, W. R. Methoxylation of Desazadesferrioxamine Analogues: Enhanced Iron Clearing Efficiency. *J. Med. Chem.* **2003**, *46*, 1470–1477.
- (40) Bergeron, R. J.; Wiegand, J.; Weimar, W. R.; Vinson, J. R. T.; Bussenius, J.; Yao, G. W.; McManis, J. S. Desazadesmethyl-desferrioxamine Analogues as Orally Effective Iron Chelators. *J. Med. Chem.* **1999**, *42*, 95–108.
- (41) Galanello, R.; Forni, G.; Jones, A.; Kelly, A.; Willemsen, A.; He, X.; Johnston, A.; Fuller, D.; Donovan, J.; Piga, A. A Dose Escalation Study of the Pharmacokinetics, Safety, and Efficacy of Deferitron, an Oral Iron Chelator in Beta Thalassemia Patients. *ASH Annu. Meet. Abstr.* **2007**, *110*, 2669.
- (42) Bergeron, R. J.; Wiegand, J.; McManis, J. S.; Vinson, J. R. T.; Yao, H.; Bharti, N.; Rocca, J. R. (S)-4,5-Dihydro-2-(2-hydroxy-4-hydroxyphenyl)-4-methyl-4-thiazolecarboxylic Acid Polyethers: A Solution to Nephrotoxicity. *J. Med. Chem.* **2006**, *49*, 2772–2783.
- (43) Bergeron, R. J.; Wiegand, J.; Bharti, N.; Singh, S.; Rocca, J. R. Impact of 3,6,9-Trioxadecyloxy Group on Desazadesferrioxamine Analogue Iron Chelators and Organ Distribution. *J. Med. Chem.* **2007**, *50*, 3302–3313.

- (44) Naegeli, H.-U.; Zähner, H. Metabolites of Microorganisms. Part 193. Ferrithiocin. *Helv. Chim. Acta* **1980**, *63*, 1400–1406.
- (45) Hahn, F. E.; McMurry, T. J.; Hugi, A.; Raymond, K. N. Coordination Chemistry of Microbial Iron Transport. 42. Structural and Spectroscopic Characterization of Diastereomeric Cr(III) and Co(III) Complexes of Desferrithiocin. *J. Am. Chem. Soc.* **1990**, *112*, 1854–1860.
- (46) Anderegg, G.; Räber, M. Metal Complex Formation of a New Siderophore Desferrithiocin and of Three Related Ligands. *J. Chem. Soc., Chem. Commun.* **1990**, 1194–1196.
- (47) Bergeron, R. J.; Wiegand, J.; Dionis, J. B.; Egli-Karmakka, M.; Frei, J.; Huxley-Tencer, A.; Peter, H. H. Evaluation of Desferrithiocin and Its Synthetic Analogues as Orally Effective Iron Chelators. *J. Med. Chem.* **1991**, *34*, 2072–2078.
- (48) Bergeron, R. J.; Streiff, R. R.; Wiegand, J.; Vinson, J. R. T.; Luchetta, G.; Evans, K. M.; Peter, H.; Jenny, H.-B. A Comparative Evaluation of Iron Clearance Models. *Ann. N.Y. Acad. Sci.* **1990**, *612*, 378–393.
- (49) Wolfe, L. C.; Nicolosi, R. J.; Renaud, M. M.; Finger, J.; Hegsted, M.; Peter, H.; Nathan, D. G. A Non-Human Primate Model for the Study of Oral Iron Chelators. *Br. J. Haematol.* **1989**, *72*, 456–461.
- (50) Sangster, J. *Octanol-Water Partition Coefficients: Fundamentals and Physical Chemistry*; John Wiley and Sons: West Sussex, England, 1997; Vol. 2.
- (51) Bergeron, R. J.; McManis, J. S.; Weimar, W. R.; Wiegand, J.; Eiler-McManis, E. Iron Chelators and Therapeutic Uses. In *Burger's Medicinal Chemistry*, 6th ed.; Abraham, D. A., Ed.; Wiley: New York, 2003; pp 479–561.
- (52) Bergeron, R. J.; Wiegand, J.; McManis, J. S.; Bharti, N.; Singh, S. Desferrithiocin Analogues and Nephrotoxicity. *J. Med. Chem.* **2008**, *51*, 5993–6004.
- (53) Bergeron, R. J.; Wiegand, J.; McManis, J. S.; Bharti, N.; Singh, S. Design, Synthesis, and Testing of Non-Nephrotoxic Desazadesferrithiocin Polyether Analogues. *J. Med. Chem.* **2008**, *51*, 3913–3923.
- (54) Bergeron, R. J.; Bharti, N.; Wiegand, J.; McManis, J. S.; Singh, S.; Abboud, K. A. The Impact of Polyether Chain Length on the Iron Clearing Efficiency and Physicochemical Properties of Desferrithiocin Analogues. *J. Med. Chem.* **2010**, *53*, 2843–2853.
- (55) Bergeron, R. J.; Wiegand, J.; Bharti, N.; McManis, J. S.; Singh, S. Desferrithiocin Analogue Iron Chelators: Iron Clearing Efficiency, Tissue Distribution, and Renal Toxicity. *Biometals* **2011**, *24*, 239–258.
- (56) Féau, C.; Klein, E.; Kerth, P.; Lebeau, L. Preparation and Optical Properties of Novel 3-Alkoxy-carbonyl Aza- and Diazacoumarins. *Synth. Commun.* **2010**, *40*, 3033–3045.
- (57) Ornelas, M. A.; Gonzalez, J.; Sach, N. W.; Richardson, P. F.; Bunker, K. D.; Linton, A.; Kephart, S. E.; Pairish, M.; Guo, C. An Efficient Synthesis of Highly Functionalized Chiral Lactams. *Tetrahedron Lett.* **2011**, *52*, 4760–4763.
- (58) Bergeron, R. J.; Bharti, N.; Singh, S.; McManis, J. S.; Wiegand, J.; Green, L. G. Vibriobactin Antibodies: A Vaccine Strategy. *J. Med. Chem.* **2009**, *52*, 3801–3813.
- (59) Marriott, J. H.; Moreno-Barber, A. M.; Hardcastle, I. R.; Rowlands, M. G.; Grimshaw, R. M.; Neidle, S.; Jarman, M. Synthesis of the Farnesyl Ether 2,3,5-Trifluoro-6-hydroxy-4-[(E,E)-3,7,11-trimethyldodeca-2,6,10-trien-1-yloxy]nitrobenzene, and Related Compounds Containing a Substituted Hydroxytrifluorophenyl Residue: Novel Inhibitors of Protein Farnesyltransferase, Geranylgeranyltransferase I and Squalene Synthase. *J. Chem. Soc., Perkin Trans.* **2000**, *1*, 4265–4278.
- (60) Piyamongkol, S.; Liu, Z. D.; Hider, R. C. Novel Synthetic Approach to 2-(1'-Hydroxyalkyl)- and 2-Amido-3-Hydroxypyridin-4-ones. *Tetrahedron* **2001**, *57*, 3479–3486.
- (61) Li, M.-J.; Kwok, W.-M.; Lam, W. H.; Tao, C.-H.; Yam, V. W.-W.; Phillips, D. L. Synthesis of Coumarin-Appended Pyridyl Tricarbonylrhenium (I) 2,2'-Bipyridyl Complexes with Oligoether Spacer and Their Fluorescence Resonance Energy Transfer Studies. *Organometallics* **2009**, *28*, 1620–1630.
- (62) Bergeron, R. J.; Wiegand, J.; Weimar, W. R.; McManis, J. S.; Smith, R. E.; Abboud, K. A. Iron Chelation Promoted by Desazadesferrithiocin Analogs: An Enantioselective Barrier. *Chirality* **2003**, *15*, 593–599.
- (63) Hoffmann, D.; Fuchs, T. C.; Henzler, T.; Matheis, K. A.; Herget, T.; Dekant, W.; Hewitt, P.; Mally, A. Evaluation of a Urinary Kidney Biomarker Panel in Rat Models of Acute and Subchronic Nephrotoxicity. *Toxicology* **2010**, *277*, 49–58.
- (64) Han, W. K.; Bailly, V.; Abichandani, R.; Thadhani, R.; Bonventre, J. V. Kidney Injury Molecule-1 (KIM-1): A Novel Biomarker for Human Renal Proximal Tubule Injury. *Kidney Int.* **2002**, *62*, 237–244.
- (65) Bonventre, J. V. Kidney Injury Molecule-1 (KIM-1): A Urinary Biomarker and Much More. *Nephrol., Dial., Transplant.* **2009**, *24*, 3265–3268.
- (66) Zhou, Y.; Vaidya, V. S.; Brown, R. P.; Zhang, J.; Rosenzweig, B. A.; Thompson, K. L.; Miller, T. J.; Bonventre, J. V.; Goering, P. L. Comparison of Kidney Injury Molecule-1 and other Nephrotoxicity Biomarkers in Urine and Kidney Following Acute Exposure to Gentamicin, Mercury, and Chromium. *Toxicol. Sci.* **2008**, *101*, 159–170.
- (67) Vaidya, V. S.; Ramirez, V.; Ichimura, T.; Bobadilla, N. A.; Bonventre, J. V. Urinary Kidney Injury Molecule-1: A Sensitive Quantitative Biomarker for Early Detection of Kidney Tubular Injury. *Am. J. Physiol. Renal Physiol.* **2006**, *290*, F517–F529.
- (68) Bailly, V.; Zhang, Z.; Meier, W.; Cate, R.; Sanicola, M.; Bonventre, J. V. Shedding of Kidney Injury Molecule-1, A Putative Adhesion Protein Involved in Renal Regeneration. *J. Biol. Chem.* **2002**, *277*, 39739–39748.
- (69) Vaidya, V. S.; Ford, G. M.; Waikar, S. S.; Wang, Y.; Clement, M. B.; Ramirez, V.; Glaab, W. E.; Troth, S. P.; Sistare, F. D.; Prozialeck, W. C.; Edwards, J. R.; Bobadilla, N. A.; Mefferd, S. C.; Bonventre, J. V. A Rapid Urine Test for Early Detection of Kidney Injury. *Kidney Int.* **2009**, *76*, 108–114.
- (70) Antech Diagnostics; <http://www.antechdiagnostics.com/> (accessed March, 2012).
- (71) Bergeron, R. J.; Streiff, R. R.; Wiegand, J.; Luchetta, G.; Creary, E. A.; Peter, H. H. A Comparison of the Iron-Clearing Properties of 1,2-Dimethyl-3-Hydroxypyrid-4-one, 1,2-Diethyl-3-Hydroxypyrid-4-one, and Deferoxamine. *Blood* **1992**, *79*, 1882–1890.
- (72) Wood, J. K.; Milner, P. F.; Pathak, U. N. The Metabolism of Iron-Dextran Given As a Total-Dose Infusion to Iron Deficient Jamaican Subjects. *Br. J. Haematol.* **1968**, *14*, 119–129.
- (73) Bergeron, R. J.; Wiegand, J.; Brittenham, G. M. HBED: A Potential Alternative to Deferoxamine for Iron-Chelating Therapy. *Blood* **1998**, *91*, 1446–1452.
- (74) Bergeron, R. J.; Wiegand, J.; Wollenweber, M.; McManis, J. S.; Algee, S. E.; Ratliff-Thompson, K. Synthesis and Biological Evaluation of Naphthyl-desferrithiocin Iron Chelators. *J. Med. Chem.* **1996**, *39*, 1575–1581.